

THE ROLE OF SEC24  
IN PROTEIN EXPORT FROM  
THE PLANT ENDOPLASMIC RETICULUM

A Thesis Submitted to the College of  
Graduate Studies and Research  
in Partial Fulfillment of the Requirements  
for the Degree in Master of Science  
at the Department of Biology  
University of Saskatchewan  
Saskatoon

By  
Luciana Renna

© Copyright Luciana Renna, March 2008. All rights reserved.

## **PERMISSION TO USE**

In presenting this thesis in partial fulfillment of the requirements for a Postgraduate degree from the University of Saskatchewan, I agree that the Libraries of this University may make it freely available for inspection. I further agree that permission for copying of this thesis in any manner, in whole or in part, for scholarly purposes may be granted by the professor or professors who supervised my thesis work or, in their absence, by the Head of the Department or the Dean of the College in which my thesis work was done. It is understood that any copying or publication or use of this thesis or parts thereof for financial gain shall not be allowed without my written permission. It is also understood that due recognition shall be given to me and to the University of Saskatchewan in any scholarly use which may be made of any material in my thesis.

Requests for permission to copy or to make other use of material in this thesis in whole or part should be addressed to:

Head of the Department of Biology

University of Saskatchewan

Saskatoon, Saskatchewan S7N 5E2

Canada

## **ABSTRACT**

Plant cells contain multiple mobile Golgi bodies. Golgi bodies receive cargo from specialized subdomains of the endoplasmic reticulum (ER), so-called ER export sites (ERES). How ERES operate in plant cells is largely uncharacterized.

In mammals and yeast, the commonly recognized ER-to-Golgi transport model asserts that protein transport between these two organelles is mediated by vesicles. Formation of these vesicles is interceded by COPII and COPI coat complexes. COPII coat proteins assemble at ERES. The minimal components of the COPII coat comprise the following proteins: the GTPase Sar1, and two large heterodimeric complexes, Sec23/24 and Sec13/31. COPII vesicles are responsible for forward (anterograde) protein traffic from the ER to the Golgi apparatus. Proteins are constantly recycled from the Golgi back to the ER through a conserved backward (retrograde) pathway mediated by COPI coat proteins. Fusion of the anterograde and retrograde carriers with target membranes is mediated by a subset of specialized proteins called soluble N-ethyl maleimide sensitive factor attachment protein receptors (SNAREs). Studies conducted in mammalian and yeast systems also concluded that ER-to-Golgi SNARE proteins and membrane cargo proteins are concentrated into COPII vesicles through a direct interaction and binding with the pre-budding complex Sec23/24-Sar1.

The COPII component distribution and their biological function in plant cells are largely uncharacterized. Therefore, through the study of the COPII protein Sec24, this work aimed (i) to investigate where and how protein transport between ER and Golgi occurs in plant cells, and (ii) to establish the importance of the

anterograde and retrograde transport equilibrium in regulating the ER protein export. To do so, live cell imaging of a fluorescent protein fusion of Sec24 was used and the dynamics of this protein chimera were followed in tobacco leaf epidermal cells. The imaging investigations were complemented by mutagenesis studies and biochemical analyses.

The obtained results indicate that in plant cells Sec24 is localized at specific regions of the ER that represent mobile units continuously joined to the Golgi apparatus. From this study the importance of the balance between the anterograde and retrograde transport in protein ER export has also emerged. I have shown in fact, that blockage of the retrograde pathway using Arf1 mutants and COPI chemical inhibitor determines the collapse of the anterograde protein trafficking from the ER to the Golgi. Moreover, this study has shown that Sec24 is capable of an interaction with the SNAREs Sed5 and Sec22. This is a forward step in our understanding of the role of Sec24 in the mechanism of cargo selection and recruitment.

## **ACKNOWLEDGEMENTS**

My life underwent positive change during the time I spent working under the supervision of Dr. Federica Brandizzi, who provided me with the tools necessary to stand alone in the fascinating, and at the same time, difficult world of science. I cannot thank her enough for all she gave me in terms of human and scientific experience.

I would also like to thank my committee members for their advice: Dr. Vipen Sawhney and Dr. Ken Wilson.

I would like to acknowledge my colleagues in the lab for their collaboration: Dr. Sally Hanton for her suggestions during my thesis writing, to Dr. Loren Matheson and Marika Rossi for their friendship and encouragement during difficult moments, and Giovanni Stefano for helping me all the time. My family and all my friends also deserve particular thanks for they were always close to me, even if physically far. I also thank the Canada Research Chair for financial support to Federica Brandizzi and the GTF award for having supported me financially.

# TABLE OF CONTENTS

PERMISSION TO USE.....	i
ABSTRACT.....	ii
ACKNOWLEDGEMENTS.....	iv
TABLE OF CONTENTS.....	v
LIST OF FIGURES.....	ix
LIST OF TABLES.....	xi
LIST OF ABBREVIATIONS.....	xii
<b>1. Introduction.....</b>	<b>1</b>
1.1 The plant early secretory pathway.....	1
1.1.1 Endoplasmic Reticulum.....	1
1.1.2 The Golgi apparatus.....	2
1.2 Nature of protein transport.....	5
1.2.1 Bulk flow versus signal mediated transport.....	5
1.3 Proteins that organize transport between ER and Golgi.....	8
1.3.1 Anterograde and retrograde transport in the early secretory pathway.....	8
1.3.1.1 COPII (coat protein complex II).....	9
1.3.1.2 COPI (coat protein complex I).....	12
1.3.1.3 ERES and proposed models for ER-to-Golgi transport in plant cells.....	13
1.3.1.4 SNARE (soluble N-ethylmaleimide-sensitive factor Attachment proteins receptor) proteins.....	15

1.4 Sec24 cargo selection and SNAREs.....	16
1.5 SNAREs interaction sites.....	17
1.6 Objectives.....	19
1.7 Significance .....	20
<b>2. Materials and Methods.....</b>	<b>21</b>
2.1 Materials.....	21
2.1.1 Biological materials.....	21
2.1.2 Solutions, enzymes, primers and chemicals.....	21
2.1.3 Growth media.....	24
2.1.4 Antibodies.....	24
2.2 Methods.....	24
2.2.1 PCR (polymerase chain reaction).....	24
2.2.2 Overlapping PCR.....	25
2.2.3 Mutations created in Sec24 .....	26
2.2.4 DNA Agarose Gel Electrophoresis.....	27
2.2.5 DNA extraction from agarose gel.....	27
2.2.6 Vector preparation.....	27
2.2.7 Ligation reaction.....	28
2.2.8 Preparation of competent <i>E. coli</i> MC1061.....	28
2.2.9 Competent <i>E. coli</i> BL21 preparation .....	29
2.2.10 Competent <i>E. coli</i> transformation.....	30
2.2.11 Competent <i>Agrobacterium tumefaciens</i> preparation.....	30
2.2.12 Plasmid DNA extraction (Minipreps).....	31

2.2.13 Competent <i>Agrobacterium tumefaciens</i> transformation.....	32
2.2.14 Transient plant transformation.....	32
2.2.15 <i>In vitro</i> protein interaction: GST pull-down.....	33
2.2.16 Leaf protein extraction.....	34
2.2.17 <i>In vitro</i> protein interaction: Histidine-pulldown.....	35
2.2.18 SDS-PAGE.....	36
2.2.19 Western blotting.....	37
2.2.20 Confocal microscopy.....	38
2.2.21 Brefeldin A (BFA) treatment .....	40
2.2.22 BFA wash-out.....	40
<b>3. Results</b> .....	41
3.1 Sec24 subcellular localization.....	41
3.2 YFPSec24 retains the functionality and interacts with Sec23 .....	43
3.3 ERES stability is influenced by the anterograde pathway.....	45
3.4 Retrograde pathway inhibition compromises ERES stability .....	47
3.4.1 Disruption of the retrograde pathway by using Arf1 mutants... 47	
3.4.2 Chemical inhibition.....	51
3.5 Biochemical support for the interaction of Sec24 with SNAREs	
interaction: Histidine pull-down for protein interaction between	
Sec24-Sed5 and Sec24-Sec22.....	55
3.6 Identification of important residues for the interaction between Sec24	
and SNAREs.....	57
3.7 Mutagenesis and sub-cellular localization of Sec24 mutants.....	59



<b>4. Discussion</b> .....	64
4.1 ERES are distributed at the peri-Golgi area in <i>N. tabacum</i> epidermal leaf cells.....	64
4.2 An equilibrium between anterograde and retrograde pathway is important for protein cycling at the ER/Golgi interface.....	66
4.3 The identification of an interaction between Sec24 and SNAREs could be the key to understand the mechanism of protein export from the ER in plants.....	68
<b>5. Conclusions</b> .....	71
<b>6. Appendix</b> .....	73
<b>7. References</b> .....	84

## LIST OF FIGURES

Figure 1.1	Schematic representations of the two models for ER export of protein .....6
Figure 1.2	Schematic diagram of COPII vesicle formation at ERES..... 11
Figure 2.1	pGEX-KG schematic representation..... 22
Figure 2.2	pET-28b schematic representation ..... 22
Figure 2.3	pVKH18En6a schematic representation .....23
Figure 2.4	pVKH18En6b schematic representation .....23
Figure 3.1	<b>ER export sites (ERES)</b> and the Golgi apparatus form secretory units..... 42
Figure 3.2	The functionality of YFPsec24 is confirmed by the interaction with the COPII component Sec23..... 44
Figure 3.3	Arrest of the anterograde pathway by the GTP mutant of Sar1 hampers the stability of the ERES... 46
Figure 3.4	Arf1GFPwt does not affect the localization of YFPsec24..... 49
Figure 3.5	Inhibition of the retrograde pathway using the Arf1 mutant blocked in the GDP form compromises ERES stability..... 49
Figure 3.6	Overexpression of the Arf1 mutant, blocked in the GTP form, compromises ERES stability ..... 50
Figure 3.7	Chemical inhibition of the COPI pathway causes

	a blockin ERES formation.....	53
Figure 3.8	The chemical block caused by BFA is completely reversible upon its elimination from the treated sample.....	54
Figure 3.9	The Histidine-pull down demonstrates an interaction between wt Sec24 with Sed5 and Sec22.....	56
Figure 3.10	A high conservation in residues involved in protein-protein interaction is found between yeast and Arabidopsis Sec24.....	58
Figure 3.11	The different subcellular localization between YFPsec24wt and YFPsec24 mutants suggest a reduced functionality of the mutated proteins compared to the wt.....	61
Figure 3.12	In presence of cargo, the recruitment of YFPsec24 Y438A is increased.....	62
Figure 3.13	In presence of cargo the recruitment of YFPsec24 V689A is increased.....	62
Figure 3.14	In presence of cargo the recruitment of YFPsec24 L749A is increased.....	63

## LIST OF TABLES

Table A1	Plasmids, <i>Agrobacterium tumefaciens</i> and <i>E. coli</i>	
	Strain.....	73
Table A2	Solutions.....	74
Table A3	Restriction endonucleases.....	78
Table A4	Primers used in PCR reactions.....	79
Table A5	Kits .....	80
Table A6	Media.....	81
Table A7	Composition of PCR reactions.....	82
Table A8	Solutions for preparing separating and stacking gels.....	83

## LIST OF ABBREVIATIONS

Arf	ADP ribosylation factor
bp	Base pair
cDNA	Complementary DNA
CASP	CCAAT-displacement-protein alternatively spliced product
CFP	Cyan fluorescent protein
COPI	Coat protein complex I
COPII	Coat protein complex II
DNA	Deoxyribonucleic acid
dNTPs	Deoxyribonucleoside triphosphates
ddH <sub>2</sub> O	Bidistilled water
ECL	Enhanced chemiluminescence
EDTA	Ethylenediaminetetraacetic acid
ER	Endoplasmic reticulum
ERD2	Endoplasmic reticulum retention defective 2
ERES	ER export sites
GAP	GTPase activating protein
GDP	Guanosine diphosphate
GEF	Guanine nucleotide exchange factor
GFP	Green fluorescent protein
GST	Glutathione S-transferases
GTP	Guanosine triphosphate
His	Histidine

IPTG	Isopropyl-beta-D-thiogalactopyranoside
Kb	Kilobase
LB	Luria Bertani
LV	Lytic vacuole
MES	2-(N-morpholino) ethane sulfonic acid 4-morpholineethanesulfonic acid
NSF	N-ethylmaleimide-sensitive factor
PBS	phosphate buffered saline
PCR	Polymerase chain reaction
Sar	Secretion associated and Ras related
SDS	Sodium dodecyl sulfate
SNAREs	Soluble N-ethyl maleimide sensitive factor attachment protein receptors
ST	Sialyl transferase
TAE	Tris-acetate-EDTA
TEMED	Tetramethylethylenediamine
TFBI	Transformation buffer I
TFBII	Transformation buffer II
TGN	Trans-Golgi network
YFP	Yellow fluorescent protein
YT	Yeast extract tryptone

## **1. INTRODUCTION**

### **1.1 The plant early secretory pathway**

The secretory pathway is a complex of endomembranes responsible for the synthesis, transport and modification of proteins, lipids and sugars (Palade, 1975; Staehelin, 1997). The main organelles of the secretory pathway are the endoplasmic reticulum (ER), the Golgi apparatus, plasma membrane and vacuoles. Vesicles shuttle cargo molecules, such as proteins, lipids, and polysaccharides, between these organelles. Proteins are synthesized on the surface of the ER and then they proceed to the Golgi apparatus (Vitale and Denecke, 1999; Neumann et al., 2003). Together, the ER and the Golgi apparatus make up the first part of the secretory pathway: the early secretory pathway. The progression of cargo from the ER to the Golgi is called the anterograde pathway. The retrograde pathway runs in the opposite direction of the anterograde, i.e. from the Golgi to the ER (Vitale and Denecke, 1999).

Over the past decade, several studies on the early secretory pathway have elucidated how proteins are exported from the ER in yeast and in mammals (Rose and Doms, 1988; Aridor et al., 2001; Hanton et al., 2005a). In plants, however, these studies are much younger (Hanton et al., 2005b; Matheson et al., 2006). For example, the function and distribution of the ER export sites (ERES) has yet to be characterized, in plants.

#### **1.1.1 Endoplasmic Reticulum**

The ER is characterized by a large membrane surface, which incorporates different types of integral and peripheral proteins, and encloses a lumen containing

soluble proteins (Staehein, 1997; Vitale and Denecke, 1999). This membrane system is in continuity with the nuclear envelope (NE) and, in plant cells, it extends through the plasmodesmata to adjacent cells (Staehein, 1997).

The presence of ribosomes on distinct areas of the ER allows the identification of two types of ER: the smooth endoplasmic reticulum (SER), without associated ribosomes, and the rough endoplasmic reticulum (RER) with associated ribosomes (Palade, 1975).

In plant cells the ER is composed of various domains, which are morphologically different and have specific functions (Staehein, 1997). The main function of the ER includes synthesis, processing and sorting of proteins, glycoproteins and lipids (Vitale and Denecke, 1999). Once the proteins are in a folded conformation, they are packaged into vesicles and exported from the ER to the Golgi apparatus (Stephens et al., 2000).

### **1.1.2 The Golgi apparatus**

Since its discovery by Camillo Golgi in 1898, the Golgi apparatus has been one of the most studied organelles. The reason for this interest is that the Golgi apparatus is involved in the secretory and endocytic pathways (Glick and Malhotra, 1998; Neumann et al., 2003). In plant cells, the Golgi is the main organelle for the synthesis of the cell wall polysaccharides and also for the production of glycolipids and glycoproteins, destined for the plasma membrane, cell wall and storage vacuoles (Neumann et al., 2003).



The Golgi apparatus is made up of a sequence of compact cisternae that are closely associated. The structure of this apparatus is polarized: the *cis* face communicates with the ER and exchanges lipids and proteins with this compartment. The *medial* Golgi which is the central Golgi domain is made of tubular and vesicular structural elements and contains specific enzymes for protein processing including the removal of mannose and the addition of N-acetylglucosamine (Griffith, 2000). Finally, the *trans* face is involved in transport to the plasma membrane (Latijhouwerrs et al., 2005). From the *cis* to the *trans* face of the Golgi stack there is a gradual change in enzymatic activities (Fitchette et al., 1999; Neumann et al., 2003). This allows a post-translational modification of the cargo as it sequentially passes through the cisternae, from the *cis* to the *trans* Golgi face. At the *trans* Golgi, secretory cargo is sorted to the final destination inside the cell.

In plants, the Golgi organization is different compared to other organisms. The Golgi apparatus in a plant cell is arranged as small cisternal stacks sprinkled in the cytoplasm in close association with the ER network.

The Golgi structure in mammalian cells has been described as a group of several stacks composed by flat cisternae interrelated by tubular networks (Rambourg and Clermont, 1990). The entire structure creates an uninterrupted membranous ribbon located at the centrosome near the apical portion of the cell surface (Thyberg and Moskalewski, 1985; Ojakian et al., 1997). In yeast cells, the organization of the Golgi has a unique aspect; it typically exhibits single layers of Golgi cisternae spread throughout the cytoplasm (Preuss et al., 1992; Rossanese et al., 1999).

Despite these differences in Golgi organization among the three cellular organisms mentioned, the conserved feature of this organelle is its dynamics, notwithstanding its structural organization, which ensures the correct modification and sorting of secretory proteins. It is generally assumed that the structure of this organelle is maintained by the presence of a matrix of resident proteins (Slusarewicz et al., 1994; Seemann et al., 2000; Renna et al., 2005).

It has been shown in mammalian cells that the maintenance of the Golgi structure is the result of a perfect equilibrium between the anterograde and retrograde membrane flow (Lippincott-Schwartz et al., 2000; Shorter and Warren, 2002). If this equilibrium is compromised, the Golgi organization is disrupted. This effect can be caused by the use of reagents, which block the organization of the ER export machinery (Shima et al., 1998; Storrie et al., 1998); or by blocking the machinery that regulates the retrograde pathway from the Golgi apparatus to the ER (Jackson et al., 1993). Drugs, like the fungal metabolite brefeldin A (BFA), interfere with the activity of Arf1 that regulates the retrograde pathway. When the drug is removed by washing, Golgi stacks promptly regenerate (Klausner et al., 1992; Satiat-Jeunemaitre and Hawes, 1992). It is unknown whether the maintenance of equilibrium between the anterograde and retrograde pathways is important for the Golgi integrity in plant cells.

## **1.2 Nature of protein transport**

### **1.2.1 Bulk flow versus signal mediated transport**

Proteins that leave the ER are either soluble or membrane anchored (Denecke et al., 1990; Benghezal et al., 2000; Phillipson et al., 2001; Contreras et al., 2004).

Two possible mechanisms are involved in the export of proteins from the ER to the Golgi: bulk flow (passive) or through a receptor mediated mechanism (Figure 1.1).

The former postulates that proteins are passively exported from the ER to the Golgi apparatus (Barlowe, 2003). The receptor mediated model assumes that cargo is selected and packaged into ER derived vesicles by a specific receptor (Barlowe, 2003; Neumann et al., 2003). It is generally assumed that, in plants, ER export of soluble proteins occurs by a passive process (bulk flow).

The export of membrane proteins from the ER is an active field of investigation. There are different classes of membrane proteins: type I, type II membrane proteins and multispinning proteins (Hanton et al., 2005b). Type I membrane proteins have their amino-terminal (N-terminal) domain in the lumen of secretory organelles, and the carboxyl-terminus (C-terminus) is exposed to the cytosol (Hampton et al., 1996). Type II proteins have the N-terminal domain exposed in the cytosol while the C-terminus remains in the lumen of the endomembrane compartment (Denzer et al., 1995; Hinnens et al., 1999; Vitale and Denecke, 1999).

Multispinning proteins are inserted into the membrane in pairs, and the topology of the protein is usually influenced by the orientation of the first hydrophobic spanning segment (Wessels and Spiess, 1988; Hinnens et al., 1999).

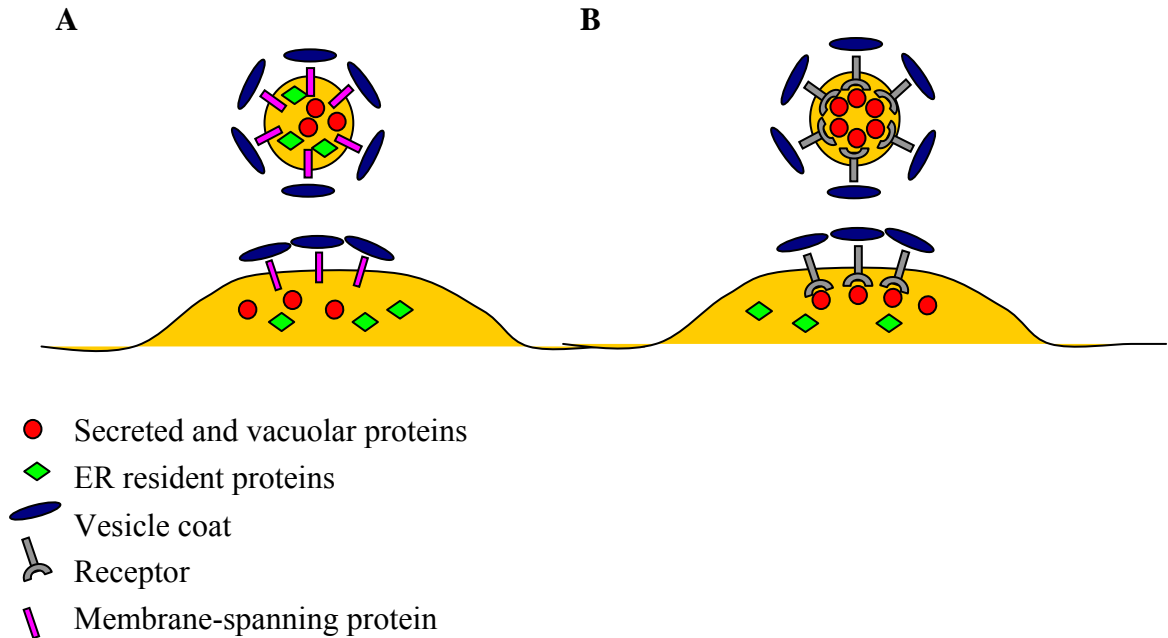


**Figure 1.1 Schematic representations of the two models for ER export of protein.**

**(A) Bulk-flow:** A membrane-spanning protein interacting with the coat promotes spontaneous vesicle budding. During this diffusive process, ER resident proteins, secreted and vacuolar proteins are packed into vesicles and exported from the ER to the Golgi apparatus. Resident ER proteins are then packaged in the Golgi and shuttled back to the ER via the retrograde pathway.

**(B) Active transport:** The formation of a vesicle coat is triggered by the binding of cargo proteins and their sorting receptor (secreted and vacuolar proteins are represented by circles). (Figure modified from Vitale and Denecke, 1999).

In plants, the destination of membrane proteins appears to be influenced by specific domains. In particular, it was found that the transmembrane portion alone of multispanning proteins is sufficient to control protein export from the ER (Hofte and Chrispeels, 1992). The destination of type I membrane protein is influenced by the length of the transmembrane domain. It has been shown that an artificial peptide with seventeen aminoacids in its transmembrane domain is retained in the ER. However, when three aminoacids were added to this transmembrane domain, the resultant protein was found in the Golgi (Brandizzi et al., 2002b). Similarly it has been hypothesized that the length of the transmembrane segment may also be important for type II and multispanning proteins (Hanton et al., 2005b). It is still unknown if ER - Golgi transport can be stimulated by the presence of a specific signal sequence contained in the transmembrane domain. Type II proteins, like CASP (CCAAT-displacement-protein alternatively spliced product) possess a tyrosine residue in the transmembrane domain that seems to be fundamental for ER-Golgi transport in mammalian cells (Gillingham et al., 2002). In plants, however, it has been shown that this tyrosine does not have the same function (Renna et al., 2005).

It has also been shown that signals in the cytosolic spanning region of membrane proteins can influence ER export. Different classes of ER export signal have been identified in the cytosolic domain of transmembrane proteins in yeast and mammalian cell systems (Kappeler et al., 1997; Nishimura and Balch, 1997; Giraudo and Maccioni, 2003). There are different types of ER export motifs. These include dihydrophobic, dibasic and diacidic motifs (Barlowe, 2003; Giraudo and

Maccioni, 2003; Hanton et al., 2005b). Diacidic motifs are composed of two acidic amino acid residues separated by any amino acid (Nishimura and Balch, 1997; Nishimura et al., 1999; Sevier et al., 2000; Ma et al., 2001; Votsmeier and Gallwitz, 2001). Studies in yeast demonstrate that the diacidic motifs interact with a component of the ER export machinery (Votsmeier and Gallwitz, 2001). Diacidic and dibasic motifs have been identified in certain transmembrane proteins plants (Contreras et al., 2004; Hanton et al., 2005b; Hawes and Satiat-Jeunemaitre, 2005; Matheson et al., 2006). Recent studies based on mutated forms of the ER export motifs of these transmembrane proteins have demonstrated the importance of these sequences for export of proteins from the ER also in plants (Hanton et al., 2005a).

### **1.3 Proteins that organize transport between ER and Golgi**

#### **1.3.1 Anterograde and retrograde transport in the early secretory pathway**

It is generally assumed that proteins are carried through the secretory pathway by vesicles (Rothman, 1994; Hanton et al., 2005a). The machinery that regulates ER export is conserved across kingdoms (Ferro-Novick and Jahn, 1994; Springer et al., 1999; Gorelick and Shugrue, 2001; Jurgens, 2004). Studies in yeast and mammals have shown that specific cytoplasmic coat protein complexes (COPs) polymerize on the membrane surface of the donor compartment and are directly involved in the mechanism of vesicle budding (Bednarek et al., 1996; Schekman and Orci, 1996). Some of these cytoplasmic coat proteins are also involved in the mechanism of selection of ER export competent cargo (Gorelick and Shugrue, 2001; Miller et al.,

2002). Vesicle budding is the final result of coat polymerization. The coating and uncoating processes of the vesicles are regulated by small GTP-binding proteins, which are members of the ARF family (Zhu et al., 1998; Bigay et al., 2003; Nie et al., 2003).

### **1.3.1.1 COPII (coat protein complex II)**

The coat protein complex responsible for ER protein export is called COPII (Aridor et al., 1999; Hammond and Glick, 2000; Aridor et al., 2001). The assembly of the COPII coat occurs at ERES (Watson et al., 2006). The ER membrane associated guanine-nucleotide exchange factor (GEF), called Sec12, is responsible for the activation and recruitment of the Sar1 GTPase (Aridor and Balch, 2000; Bi et al., 2002). Upon activation, Sar1 (Sar1GTP) recruits two protein complexes to the ER membrane. The first complex is made of two proteins: Sec23 that possesses GTPase-activating protein activity (GAP) and Sec24 that is important for cargo selection and recruitment (Aridor et al., 2001). The Sec23/24-Sar1 complex is believed to select cargo in order to form the so-called pre-budding complex (Figure 1.2) (Barlowe et al., 1994; Matsuoka et al., 2001; Mancias and Goldberg, 2005). During this process, soluble N-ethyl maleimide sensitive factor attachment protein receptors (SNAREs), which mediate vesicle fusion with the Golgi (Parlati et al., 2000; Parlati et al., 2002), are also packaged into COPII vesicles (Kuehn et al., 1998). Once the pre-budding complex is complete, Sec23/Sec24-Sar1 recruits the second heterodimer, Sec13/31 which cross-links the pre-budding complex (Schekman and Orci, 1996; Antonny et al., 2001; Lee et al., 2004) (Fig 1.2). The

Sec13/31 heterodimer is also responsible for driving membrane deformation (Barlowe, 2003; McMahon and Mills, 2004; Mancias and Goldberg, 2005). At this stage, the GAP activity of Sec23 converts Sar1GTP into the inactive form Sar1 GDP by stimulating Sar1GTP hydrolysis (Yoshihisa et al., 1993). Once Sar1 is in the inactive state, the COPII coat is released to the cytosol and the vesicle containing proteins buds from the ER membrane. Despite the conservation of coat components across eukaryotic cell systems, the study of COPII proteins is in its infancy in plants.

It has been shown that over-expression of a mutant of Sar1 that blocks the GTPase in its active state (Sar1-GTP), initiates the collapse of the ER-to-Golgi protein transport in plant cells (Andreeva et al., 2000; Takeuchi et al., 2000; Phillipson et al., 2001; daSilva et al., 2004). This confirms that COPII proteins participate in ER-to-Golgi protein transport in plants.

DaSilva et al. (2004) have demonstrated that a yellow fluorescent protein (YFP) fusion of Sar1 (Sar1-YFP) is usually distributed in the cytosol. When secretion was stimulated by over-expression of membrane proteins, such as ERD2-GFP (endoplasmic reticulum retention defective 2 protein) and ST-GFP (sialyl transferase protein), which shuttle between the ER and Golgi (Brandizzi et al., 2002b), Sar1-YFP was distributed to punctate structures at the peri Golgi area. This study concluded that Sar1 localizes at ERES and also demonstrated that ERES formation is induced by the presence of ER export competent cargo (daSilva et al., 2004; Hanton et al., 2005a; Stefano et al., 2006; Hanton et al., 2007).



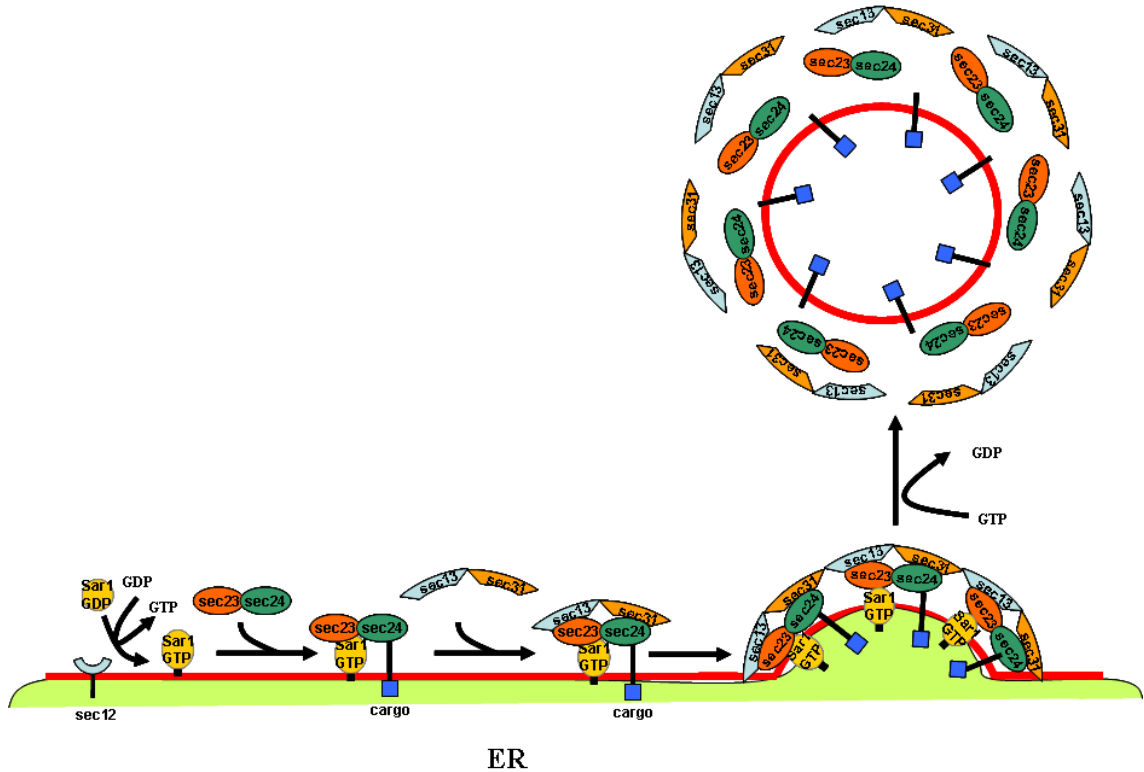


**Figure 1.2: Schematic diagram of COPII vesicle formation at ERES.**

Sec12 (the guanidine exchange factor) activates and recruits the GTPase Sar1.

Once converted to the GTP form, Sar1GTP recruits the heterodimeric complex Sec23/24.

This pre-budding complex is able to select the cargo ready to be exported from the ER.

Another heterodimeric complex Sec13/31 at this stage is recruited from the pre-budding complex already formed. This completes the coat and also provides the driving force for vesicle budding. Sec23 with its GAP activity converts Sar1GTP into Sar1GDP. All the coat components are then released as is the vesicle which is free to go in the cytoplasm or to fuse to other organelles. (Figure modified from Mancias and Goldberg, 2005).

It is still unknown whether Sar1 is directly or indirectly involved in the recruitment and selection of membrane proteins at ERES through the interaction with specific signal sequences present in the cytosolic tail, as has been suggested in other systems (Aridor et al., 1998; Springer and Schekman, 1998; Giraudo and Maccioni, 2003). It is also unknown whether the other COPII proteins such as Sec23/24 and Sec13/31 are recruited to the ER when membrane secretory cargo is over-expressed or whether this is a specific feature of Sar1.

### **1.3.1.2 COPI (coat protein complex 1)**

The COPI protein complex regulates the retrograde pathway to transport proteins from the Golgi to the ER. The presence of COPI-coated vesicles has been demonstrated in mammalian (Waters et al., 1991), yeast (Duden et al., 1994), and plant cells (Pimpl et al., 2000). The COPI complex is composed of 7 subunits:  $\alpha$ ,  $\beta$ ,  $\beta'$ ,  $\gamma$ ,  $\delta$ ,  $\zeta$  COP (Waters et al., 1991) and Arf1, a small GTPase (Donaldson et al., 1992b; Palmer et al., 1993). In *Arabidopsis* there are homologues of these proteins (Contreras et al., 2000; Pimpl et al., 2000). Mammalian and yeast ARFs have conserved functional regions that are present in the twelve ARFs encoded by the *Arabidopsis* genome (Gebbie et al., 2005).

The first step of coatomer formation is the conversion of Arf1GDP (inactive form) into Arf1GTP (active form) by the action of a GEF (Donaldson et al., 1992b; Helms and Rothman, 1992). Arf1GTP binds Golgi membranes and recruits the other COPI subunits from the cytosol. Once assembled on Golgi membranes, the COPI

coat induces membrane curvature and promotes vesicle budding (Puertollano et al., 2001).

A GAP protein is responsible for the hydrolysis of GTP, converting Arf1GTP into Arf1GDP (Nie et al., 2003; Memon, 2004; Wennerberg et al., 2005). In the GDP/ inactive state, ARF1 dissociates from the membrane and the vesicle is released (Mossessova et al., 2003b; McMahon and Mills, 2004).

It has been shown in mammalian cells that disruption of the COPI activity via specific drugs such as brefeldin A do not affect recruitment of COPII coat to ERES (Ward et al., 2001). Whether this is the case also in plants is yet to be determined.

### **1.3.1.3 ERES and proposed models for ER-to-Golgi transport in plant cells**

ERES are regions of the ER where COPII vesicles are assembled and proteins that have to be exported to the Golgi are sorted (Orci et al., 1991; Barlowe et al., 1994; Barlowe, 2002; Stephens and Pepperkok, 2004).

ERES of different cell types and different organisms show different features. In vertebrate cells, they resemble vesicular structures on ER domains that are concentrated at the perinuclear region, where the Golgi apparatus is located (Palade, 1975). In some yeast, ERES containing COPII coat proteins and Sec12 are distributed next to the Golgi stacks (Rossanese et al., 1999). In plant cells, ERES morphology and distribution are a matter of recent debate. To date, three models that explain ER-to-Golgi protein export have been proposed. The first model, so called ‘vacuum cleaner model’, was hypothesized in 1998 (Boevink et al., 1998). It

was suggested that Golgi stacks move along the ER surface sweeping up export vesicles that bud from the ER continuously. No experimental data have been produced to support this model. The second model is known as ‘stop and go’ or ‘kiss and go’ (Nebenfür et al., 1999). This model suggests that Golgi bodies move on the ER surface and that the Golgi stops on spatially-fixed ERES present on the ER surface and collects cargo.

The third model was established on the analysis of the dynamics of a fluorescent fusion of Sar1, the GTPase that initiates COPII assembly at ERES (daSilva et al., 2004). Sar1 was found to label ER domains in close association with Golgi bodies. This observation lead to a model that suggests the existence of a mobile ERES that travels as a single unit with a Golgi body over the ER.

A recent publication based on the dynamics of a fluorescent fusion of the COPII protein Sec13, has shown that Sec13 positive structures are free in the cytosol and sometimes they associate with Golgi bodies (Yang et al., 2005). The model generated in this work hypothesized that a Golgi body can be attached to different ERES at the same time and that this association is only transient. These data support the ‘stop and go’ model.

It is possible that the discrepancies between the models proposed by da Silva et al (2004) and Yang et al. (2005) are due to the distribution of the two different COPII markers used in the studies. Therefore, an analysis of the dynamics of an additional COPII marker may shed light on the distribution of ERES and mechanisms of ER-to-Golgi protein transport in plant cells.

#### **1.3.1.4 SNARE (soluble N-ethylmaleimide-sensitive factor attachment proteins receptor) proteins**

To transport successfully cargo between organelles within the secretory pathway, transport vesicles generated on a donor organelle have to fuse with the membrane of an acceptor organelle. A class of proteins called SNAREs has been implicated in such a membrane targeting fusion process (Hong, 2005). SNAREs are conserved among all eukaryotes (Jahn et al., 2003; Pratelli et al., 2004). The structure of these proteins is very simple (Ungar and Hughson, 2003); they are type II membrane anchored proteins and contain one or multiple SNARE motifs in the cytosolic domain. These motifs consist of repeating heptads (60-70 amino-acids) of hydrophobic residues. The spacing of these hydrophobic residues is organized in such a manner that an  $\alpha$ -helical structure exposes all the hydrophobic side chains on the same side of the helix. The SNARE transmembrane domain engages the membrane substrate necessary for and directly involved in membrane fusion, promoting bilayer mixing and also regulating the SNARE localization (Ungar and Hughson, 2003).

One of the first classifications of SNAREs was based on studies on neuronal cells (Sollner et al., 1993). SNAREs were classified as t- or v- SNAREs. T-SNAREs are localized on the membrane of the target organelle, and v-SNAREs are localized on the membrane of the vesicle budding from the donor organelle.

Membrane fusion mechanisms require that a v-SNARE and a t-SNARE interact at the vesicle/membrane interface of the target organelle and form a stable complex (Weber et al., 1998; Chen et al., 1999). This complex is important to

initiate the fusion of the vesicle membrane with that of the acceptor organelle. Once the fusion is complete, the SNARE complex is disassembled. The disassembling of the SNARE complex necessitates a specialized machinery, which is made up of the chaperone NSF (N-ethylmaleimide-sensitive fusion protein) and the co-chaperone SNAP (soluble NSF attachment protein) (Sollner et al., 1993). When the complex is disassembled SNAREs are released. The v-SNAREs are then recycled back to their original location to be used again.

In *Homo sapiens*, *Drosophila melanogaster* and *Saccharomyces cerevisiae*, more than 35 genes coding for SNAREs have been identified. In *A. thaliana*, analysis of the genome has established the presence of 54 SNARE genes (Sanderfoot et al., 2000; Uemura et al., 2004).

#### **1.4 Sec24 cargo selection and SNAREs**

In yeast cells, it is thought that the specific recruitment of membrane cargo is based on the direct interaction between the cytosolic domain of the cargo and the COPII coat components (Schekman and Orci, 1996). To date, little is known about the relationship between cargo and coat proteins in plants.

Sec24, one of the COPII coat components, seems to be directly involved in the cargo selection process in non plant systems such as yeast and mammals (Aridor et al., 1998), upon interaction with ER export signals present in the cytosolic tail of certain cargo proteins (Miller et al., 2002). In particular in yeast, it has also been shown that diacidic export motifs of TMD (membrane) cargo can interact with the Sec23/24 complex (Aridor et al., 2001; Votsmeier and Gallwitz, 2001). Mutagenesis

of the diacidic region of Sys1p reduced the Sec23/24 interaction, resulting in a decrease in the incorporation of cargo molecules into COPII vesicles (Miller et al., 2003).

Studies using synthetic liposomes showed that a homologue of Sec24, Lst1p, is needed for the transport of specific cargo molecules through the secretory pathway, such as the plasma membrane ATPase (Roberg et al., 1999; Shimoni et al., 2000). This discovery supports the role of Sec24 in cargo selection (Roberg et al., 1999; Shimoni et al., 2000; Barlowe, 2003).

The role of Sec24 in ER protein export is unknown in plants. In particular, it is not known where this protein is localized nor it is understood whether Sec24 is involved in the process of cargo selection.

### **1.5 SNAREs interaction sites**

Studies using *S. cerevisiae* have shown that the SNARE complex required for ER-Golgi transport is formed by the t-SNAREs Sed5 (syntaxin5), Bos1, and Sec22 and the associated v-SNARE Bet1. This complex of t- and v- SNARE is called fusogenic, because it predisposes membrane fusion (Newman et al., 1990; Dascher et al., 1991; Hardwick and Pelham, 1992; Parlati et al., 2000). Arabidopsis homologues of Sed5, Bos1, and Sec22 have been shown to have a role in ER export in plants (Chatre et al., 2005).

By a crystallographic analysis of the Sec24 structure, it has been shown that Sec24 contains three domains that may be involved in SNARE recognition, these have been indicated as A-site, B-site, and C-site. A-site is able to recognize a

YNNSNPF sequence in Sed5 (Mossessova et al., 2003a). The B-site of Sec24 recognizes an LXXL/ME motif in Bet1 and Sed5 (Mossessova et al., 2003a). The C-site, which includes Arginine 342, recognizes Sec22 (Miller et al., 2003). Moreover, it has been demonstrated that the t-SNARE Sed5 cycles through the ER and Golgi (Wooding and Pelham, 1998), and an interaction between Sed5 and Sec24 may be necessary during the cargo selection process (Peng et al., 1999; Miller et al., 2005).

To date, it is yet unknown whether Sec24 also recognizes SNAREs in plants and whether a Sec24-SNARE interaction has a role in protein export from the plant ER.



## 1.6 Objectives

The aim of this research is to gather insights into the molecular mechanisms for protein export at ERES in plants. The hypothesis is that Sec24 is involved in ER-to-Golgi transport in plant cells. This protein has been extensively characterized in non-plant systems, but its function and distribution in plants are unknown.

Specifically, the objectives are:

- To determine where Sec24 is distributed in plant cells.
- To understand how ERES and Golgi are related during ER to Golgi protein transport.
- To understand the relevance of an equilibrium between COPI and COPII activity for the process of protein transport between the ER and Golgi apparatus.
- To investigate the existence of an interaction between Sec24 and different SNARE proteins.
- To identify and mutate the sites involved in the interaction between Sec24 and SNAREs.
- To understand how cargo selection is regulated and the possible role of SNAREs in the mechanisms of cargo selection and cargo export from the ER to the Golgi.

To achieve these objectives tobacco leaf epidermal cells were used as an experimental system due to their amenability to transformation. Live cell imaging coupled with molecular cloning and biochemical analyses were utilized as experimental tools.

## **1.7 Significance**

Achieving the objectives in this thesis will advance our understanding of the basic mechanisms that govern ER export in plants. Protein export is an important issue not only for the life of plant cells but also for the other organisms that survive on proteins that are produced by the plant secretory pathway. A better understanding of how plants manage to produce and store secretory products may increase our ability to exploit plants as biotechnological factories.

## **2. MATERIALS AND METHODS**

### **2.1 Materials**

#### **2.1.1 Biological materials**

*Nicotiana tabacum* (cv Petit Havana) greenhouse plants were grown in a Sungro Horticulture Mix-1 Canada soil. The growth chamber equipped with cool white fluorescent light bulb was set at 25°C with a 16-hr light and 8-hr dark regime, at a light irradiance of 200  $\mu\text{E}\cdot\text{m}^{-2}\cdot\text{sec}^{-1}$ . The plasmids, *Agrobacterium tumefaciens* and *Escherichia coli* strains used in this work, are listed in the appendix, Table A1. The multiple cloning sites of different plasmids are shown in Figure 2.1-2.4. The cDNA for Sec24 and Sec23 (At3g07100 and At3g23660 respectively) was purchased from ABRC ([www.arabidopsis.org](http://www.arabidopsis.org)).

#### **2.1.2 Solutions, enzymes, primers and chemicals**

The solutions, enzymes and primers used in this research are listed in the appendix, Table A2, A3, A4, respectively. The kits used in this work are listed in Table A5. All other chemical reagents were purchased from VWR International ([www.vwr.com](http://www.vwr.com)), Sigma Aldrich ([www.sigma-aldrich.com](http://www.sigma-aldrich.com)), Bioshop Canada Inc. ([www.bioshopcanada.com](http://www.bioshopcanada.com)) and Fermentas ([www.fermentas.com](http://www.fermentas.com)).

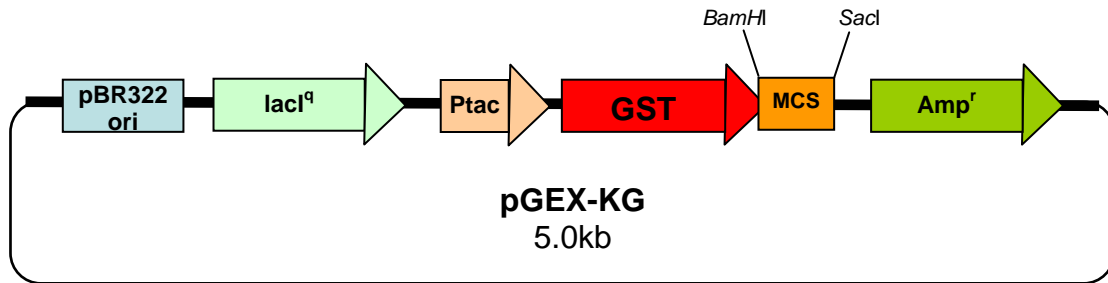


**Figure 2.1 pGEX-KG schematic representation.** This plasmid contains the gene encoding for the resistance to the ampicillin ( $Amp^R$ ), pBR322 origin which dictates low copy replication and preservation of the plasmid in *E. coli*, lacI gene encoding the lac repressor, the tac promoter/operator (Ptac), which is inducible by IPTG (Isopropyl-beta-D-thiogalactopyranoside), the glutathione S-transferase gene (GST) and the multiple cloning site (MCS).

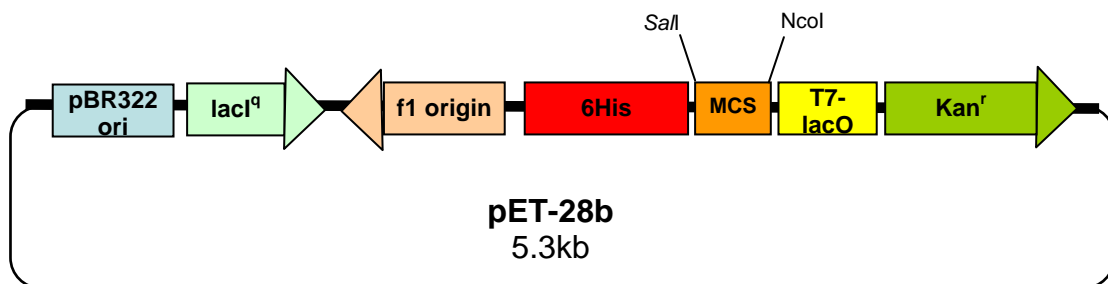


**Figure 2.2 pET-28b schematic representation.** This plasmid carries the gene encoding for the resistance to the kanamycin ( $Kan^R$ ), pBR322 origin which dictates low copy replication for the maintenance of the plasmid in *E. coli*, lacI gene encoding the lac repressor, the f1 origin of replication for the assembly of single stranded plasmid DNA, a Histidine tag sequence (6His), a multiple cloning site (MCS), and the T7-lacO promoter.

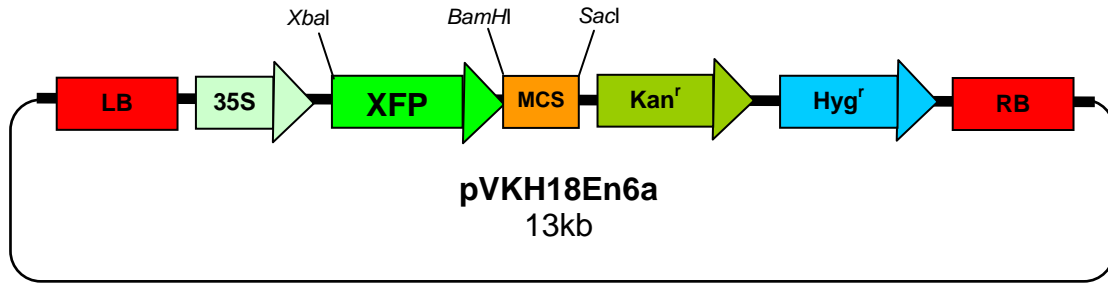


**Figure 2.3 pVKH18En6a schematic representation.** This plasmid carries the gene for kanamycin resistance ( $\text{Kan}^r$  for selection in bacteria), the gene encoding for hygromycin resistance ( $\text{Hyg}^r$  for selection in plants), the right border (RB) and the left border (LB) flanking the T-DNA, the 35S promoter, a multiple cloning site (MCS) and the gene encoding a fluorescent protein (XFP, that can be GFP/YFP/CFP respectively green/yellow and cyan fluorescent protein) at the N-terminus of the MCS.

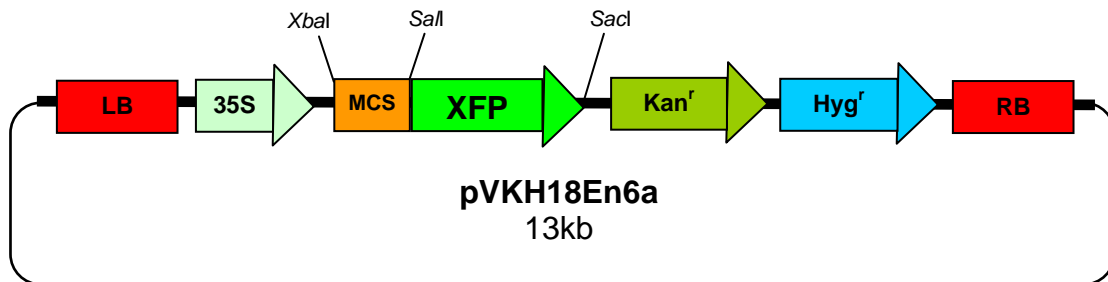


**Figure 2.4 pVKH18En6b schematic representation.** This plasmid carries the gene for kanamycin resistance ( $\text{Kan}^r$  for selection in bacteria), the gene encoding for hygromycin resistance ( $\text{Hyg}^r$  for selection in plants), right border (RB) and the left border (LB) bordering the T-DNA, the 35S promoter, a multiple cloning site (MCS), and the gene encoding a fluorescent protein (XFP, can be GFP/YFP/CFP) at the MCS C-terminal.

### **2.1.3 Growth media**

The formulations of the growth media used in this study are listed in the appendix, Table A6. LB (Luria Bertani) medium was used to grow *E. coli* and *A. tumefaciens*. Antibiotics were included in the medium to select specific resistances. YT medium was used only to grow *E. coli* MC1061 as a source of chemically competent cells for transformation.

### **2.1.4 Antibodies**

The antibodies used in this work were purchased from Abcam or Santa Cruz biotechnology. In particular, anti-GFP and anti-GST were purchased from Abcam ([www.abcam.com](http://www.abcam.com)). The anti-His and the secondary antibody (goat anti-rabbit linked to horseradish peroxidase) were purchased from Santa Cruz biotechnology ([www.scbt.com](http://www.scbt.com)). The dilutions of the antibodies used in this work were: anti-GFP at 1:2000; anti-GST at 1:500; anti-His at 1:200 and secondary antibody at 1:5000.

## **2.2 Methods**

### **2.2.1 PCR (Polymerase Chain Reaction)**

All the PCR reactions were set up as described in the appendix, Table A7. The PCRs were carried out in a Thermo Electron Corporation -PX2 Thermal Cycler ([www.thermo.com](http://www.thermo.com)), by using the program “active tube”. The reaction conditions used are described below.

Initially the DNA template was denatured by incubating the mixture at 94 °C for 4 minutes. The successive steps consisted of 3 stages: the first stage was a

denaturation stage carried at 94 °C for 30 seconds. The following stage was the annealing phase, usually between 48-55 °C for 30-45 seconds (depending on the melting temperature of the primers). The last stage of the second step was an extending step performed at 72 °C for 1 minute for the synthesis of PCR fragments of 1000 bp, by using Pfu Polymerase. Step 2 was carried out for 20 cycles. Finally there was the extending step to fill in the protruding ends of newly synthesized PCR products, performed at 72 °C for 5 minutes.

The PCR reactions were left at 4 °C until analysis by gel electrophoresis (refer to section 2.2.2). The sequences of the primers used in this study are listed in Table A4.

### **2.2.2 Overlapping PCR**

Overlapping PCR was used to insert site direct mutations in the cDNA. This method involved the use of primers containing specific alterations in the nucleotide sequence and PCR, to generate two DNA fragments. These fragments were produced in separate PCR reactions and they had overlapping ends (Higuchi et al., 1988; Ho et al., 1989). Subsequently the fragments were purified by DNA extraction from agarose gel, as described in section 2.2.5. The two products with overlapping ends were used in a subsequent PCR as new template DNA, and amplified by using the two non-mutagenic primer in 5' and 3'. All the mutants used in this work were created by this technique of site-directed mutagenesis.

### **2.2.3 Mutations created in Sec24**

Mutations were produced by using the following overlap PCR reactions (the sequences of all the primers listed are in Table A4):

1) Sec24Y438A was generated from Sec24 by using the primers 5'FB276 and 3'LR7 to amplify the first region, then the primers 5'LR6 and 3'FB278 were used to amplify the last region. Fragments were purified by agarose gel electrophoresis and were used as a new DNA template to be overlapped by the primers 5'FB276 and 3'FB278, which was then inserted into a binary vector pVKH18En6.

2) Sec24V689A was generated from Sec24 by using the primers 5'FB276 and 3'LR9 to amplify the first region, then the primers 5'LR8 and 3'FB278 were used to amplify the last region. Fragments were purified by agarose gel electrophoresis and were used as new DNA templates to be overlapped as described for Sec24Y438A.

3) Sec24L749A was generated from Sec24 by using the primers 5'FB276 and 3'LR11 to amplify the first region, then the primers 5'LR10 and 3'FB278 were used to amplify the last region. Fragments were purified by agarose gel electrophoresis and were used as new DNA templates to be overlapped as described for Sec24Y438A.

The insertion of mutations was confirmed with an automated DNA sequencer at the Department of Biology, supplied by Dr. Cota Sanchez's lab, and the data were processed by using Chromas Lite software ([www.technelysium.com.au/chromas.html](http://www.technelysium.com.au/chromas.html)).



#### **2.2.4 DNA Agarose Gel Electrophoresis**

Agarose gel electrophoresis was used to separate, visualize and analyze DNA. This allows quantification of the DNA, or to extract a particular fragment after digestion. Gels were prepared at 1% (for 50 mL: 0.5 g of agarose melted in 1X TAE buffer in a microwave and ethidium bromide added to a final concentration of 0.5 µg/ml). 1x TAE buffer was used to cover the gel and to run the samples prepared by adding 1/5 the volume of 5x loading buffer. A voltage of 100 V was used to run the electrophoresis of the samples for approximately 20-30 minutes.

#### **2.2.5 DNA extraction from agarose gel**

To extract the band of interest from agarose gel, the gel was placed on a transilluminator equipped with UV light (302 nm). The band of interest was gently excised by a razor blade and placed in a 1.5 mL eppendorf tube. DNA fragments were extracted from agarose gels by using a GFX PCR DNA & Gel Band Purification Kit (Amersham Biosciences) according to the manufacturer's instructions.

#### **2.2.6 Vector preparation**

Plasmids PVKH18EN6a, PVKH18EN6b, pET28b and pGEX were digested with restriction endonucleases (Fermentas) for cloning different cDNA sequences. In particular, PVKH18EN6a, and PVKH18EN6b were digested with *Bam*HI-*Sac*I; pET28b with *Xba*I-*Sal*I or *Nco*I-*Sal*I; pGEX with *Bam*HI-*Sac*I. The endonuclease restriction reagent was composed as follows: 0.5 µg of DNA, 10 X reaction buffer,

40 units restriction enzyme, and sterile distilled water to 100  $\mu$ L total volume. The reaction was incubated at 37  $^{\circ}$ C for 1.5 hours. The DNA was then purified by using GFX PCR purification DNA kit (Amersham biosciences). Subsequently, the plasmid was subjected to a second digestion with the other enzyme to complete the preparation of the cloning vector. After the incubation at 37  $^{\circ}$ C for 1.5 hours, the vector was loaded on an agarose gel and purified, as described in section 2.2.4.

### **2.2.7 Ligation reaction**

The ligation reaction required a clean open vector and a DNA insert previously digested with the appropriate restriction enzymes. The standard ligation reaction mixture was performed in a final volume of 20  $\mu$ L, by using (a) ligation buffer 1x purchased from GIBCO, 1 unit of T4 DNA ligase ([www.invitrogen.com](http://www.invitrogen.com)), the clean open vector, and the insert cut and cleaned (vector : insert, molar ratio = 1 : 4). The mixture was incubated at 16  $^{\circ}$ C overnight in a Thermo Electron Corporation -PX2 Thermal Cycler.

### **2.2.8 Preparation of competent *E. coli* MC1061**

*E. coli* MC1061 was streaked on LB plates containing streptomycin (final concentration 50  $\mu$ g/mL), and subjected to an overnight incubation at 37  $^{\circ}$ C. One colony was then used for an inoculate YT medium (3 mL) and the liquid culture was then grown at 37  $^{\circ}$ C with shaking at 200 rpm until an optical density of 0.300 (measured at  $\lambda= 550$  (O.D.<sub>550</sub>)) was obtained. Then, the 3 mL culture was used to inoculate 200 mL of YT medium, previously warmed to 37  $^{\circ}$ C and incubated with

shaking at 200 rpm at 37 °C. The culture was left to grow under these conditions until an O.D.<sub>550</sub> of 0.480 and then divided into four sterile 50 mL Falcon tubes (BD Falcon) and left on ice for 5 minutes. A pellet of cells was obtained by centrifuging at 3000g in a centrifuge (Beckman Avanti J-26), equipped with a JA 25.50 rotor at 4 °C for 20 minutes. The supernatant was eliminated, the pellet was resuspended in a total of 80 mL ice-cold TFB I buffer and the cells were placed on ice for 5 minutes. After a second centrifugation using the same conditions as described above, the pellet was resuspended in 8 mL of TFBII buffer and left on ice for 15 minutes. The culture was then divided into 100 µL aliquots by using pre-chilled Eppendorf tubes, and the aliquots were subsequently frozen in N<sub>2</sub> liquid and stored at -80 °C.

### **2.2.9 Competent *E. coli* BL21 preparation**

BL21 *E. coli* cells were streaked on an LB plate containing 50 mg/mL of streptomycin. After an overnight incubation at 37 °C, a single colony was inoculated into 5 mL of LB medium and grown overnight at 37 °C with 200 rpm shaking. The next day, 3 mL of this overnight culture were poured into a 250 mL sterile flask, containing 50 mL of LB and grown until an OD<sub>590</sub> of 0.5, by shaking at 200 rpm at 37 °C. Then, the culture was transferred into 50 mL sterile Falcon tubes and chilled on ice for 15 minutes. Cells were then centrifuged at 5000 rpm at 4 °C for 20 minutes, and the pellet was resuspended in 50 mL of pre-chilled 20 mM CaCl<sub>2</sub> solution and centrifuged again at 5000 rpm for 10 minutes. The new pellet was resuspended in 20 mL of pre-chilled CaCl<sub>2</sub> solution, left on ice for 30 minutes and centrifuged again at 5000 rpm for 10 minutes. Finally, the pellet was resuspended in

1 mL of CaCl<sub>2</sub> solution, divided in 100 µL aliquots in pre-chilled, sterile Eppendorf tubes and stored at -80 °C.

#### **2.2.10 Competent *E. coli* transformation**

To transform *E. coli* competent cells, a heat shock procedure was used. Aliquots of competent cells (*E. coli* MC1061 or *E. coli* BL21) were taken out of the -80°C freezer and put on ice to thaw. Once thawed, the DNA was added to the cells. To transform *E. coli* MC1061, either 10 ng of miniprep DNA or 10 ng of a ligation DNA was used. To transform *E. coli* BL21 between 30 and 50 ng of miniprep DNA was used. Once the DNA was added to the cells and mixed by pipetting up and down twice, the mixture was left on ice for about 20 minutes. After that, heat was applied to the cell suspension at 42 °C for 30 seconds and quickly transferred on ice for 5 minutes; 800 µL of LB medium were added to each tube and the cells were incubated at 37 °C with shaking at 170 rpm for 1 hour. The cell suspension was then plated on an LB agar plate, containing the specific antibiotic for the selection of the plasmid used for the transformation, and grown overnight at 37 °C.

#### **2.2.11 Competent *Agrobacterium tumefaciens* preparation**

*A. tumefaciens* (GV3101) was streaked on an LB agar plate containing an antibiotic for the selection of this bacterium (gentamycin 15 µg/mL). The plate was incubated for 48 hours at 28 °C and a single colony from the plate was inoculated into 5 mL of LB medium (with gentamycin at 15 µg/mL), and the culture was shaken overnight at 250 rpm at 28 °C. Then, 2 mL from this culture were transferred

to a sterile 250 mL flask containing 50 mL of LB plus gentamycin 15 µg/mL, and left to grow in a shaker at 250 rpm and 28 °C, until an optical density (OD<sub>600</sub>) between 0.5 and 1.0 was obtained. Cells were then transferred to 50 mL Falcon tubes and incubated on ice for 10 minutes.

Subsequently, cells were centrifuged for 10 minutes at 5000 rpm at 4°C; the pellet was then resuspended in 1 mL of sterile cold 20 mM CaCl<sub>2</sub>. The suspension was then divided in aliquots of 40 µL and immediately frozen in liquid nitrogen and stored at -80°C.

#### **2.2.12 Plasmidic DNA extraction (Minipreps)**

To extract plasmid DNA from transformed *E. coli* cells, a single colony was picked from the plate and inoculated into 3 mL of LB containing the appropriate antibiotic for the plasmid selection. The culture was grown overnight at 37 °C with agitation at 180 rpm. The 3 mL cell suspension was centrifuged at 13000 rpm at 4 °C into two steps, by transferring the culture to a 1.5 mL Eppendorf tube. After the supernatant elimination, the pellet was resuspended in 250 µL of P1 solution with 50 µg/mL of RNase A (Fermentas) (stock: 10 mg/mL in ddH<sub>2</sub>O) and left at room temperature for 15 minutes. 250 µL of P2 solution was added, gently mixed and left at room temperature no longer than 5 minutes. This step was followed by the addition of 350 µL of cold P3 solution and gently mixed. The mixture was incubated on ice for 10 minutes and centrifuged at 14000 rpm for 10 minutes at 4 °C. After the centrifugation, a clear supernatant and a white pellet were obtained; the supernatant was retained and transferred to a new Eppendorf tube containing

750  $\mu$ L of isopropanol, mixed and centrifuged at 14000 rpm at 4 °C for 30 minutes. To eliminate the isopropanol, the pellet was left to dry at 37 °C for 10 minutes, and then resuspended in 50  $\mu$ L of fresh distilled, sterile water, and stored at -20 °C.

### **2.2.13 Competent *Agrobacterium tumefaciens* transformation**

A frozen aliquot of competent *A. tumefaciens* was taken from -80 °C and left to thaw on ice. Then, 7  $\mu$ L of DNA were added, left on ice for 5 minutes, transferred to liquid nitrogen for 5 minutes, and incubated at 37 °C for other 5 minutes.

Subsequently, 800  $\mu$ L of LB medium were added. After this heat-shock treatment, cells were incubated with agitation at 130 rpm for 4 hours at 28 °C, and plated on LB plates containing gentamycin 25  $\mu$ g/mL plus the antibiotic for the plasmid selection. Plates were incubated at 28 °C for two days.

### **2.2.14 Transient plant transformation**

Four week old *N. tabacum* plants were used for *A. tumefaciens* [strain GV3101]-mediated transient expression, as previously described (Batoko et al., 2000). The agro-infiltration was performed as follows: 3 mL of *A. tumefaciens* culture were grown at 28 °C in LB containing kanamycin (100  $\mu$ g/mL) and gentamycin (25  $\mu$ g/mL) shaking at 180 rpm for about 20 hours. 1 mL of bacterial cells was centrifuged at 8000 g for 5 minutes at room temperature and then resuspended in infiltration (IF) buffer. Subsequently, it was re-centrifuged and re-suspended in 1 mL of fresh IF buffer. A spectrophotometer was used to read the optical density of the bacterial mixture at 600 nm. The optical density (OD<sub>600</sub>) used for plant

transformations was 0.05 for Sec24 and its mutants, and 0.2 for ERD2 constructs. The *Agrobacterium* was resuspended in IF medium and was injected in the tobacco leaf through the abaxial air space by using a sterile 1 mL syringe without a needle (Kapila et al., 1997).

#### **2.2.15 *In vitro* protein interaction: GST-pull down**

The sequence of Sec23 was subcloned into the expression vector pGEX, which contains a region coding for glutathione S-transferase (GST) at the beginning of the polylinker. The presence of the GST in the polylinker results in the addition of GST to the N-terminus of the cDNA of the protein of interest inserted in the vector. GST-Sec23 clones were used to transform the *E.coli* BL21 strain for protein expression. A single colony was inoculated into 5 mL of LB containing ampicillin (100 µg/mL), and shaken at 180 rpm for 15 hours at 37 °C. Then 3 mL were taken from the overnight culture and poured into a 250 mL sterile flask, containing 100 mL of LB medium with antibiotic, and shaken at 230 rpm at 30 °C until an OD<sub>600</sub> = 1.0 was reached. Recombinant protein expression was induced by the addition of 1 mM IPTG (isopropyl-beta-D-thiogalactopyranoside). The maximum amount of protein was usually achieved after 5 hours of agitation at 230 rpm at 30 °C. Successively, the culture was centrifuged at 5000 rpm for 10 minutes at 4 °C and the pellet was stored at -20 °C until further use. The pellet was then resuspended in GST-extraction buffer (1 mL/10 mL *E. coli* culture) by disrupting the cells with sonication at 15 W for 10 seconds incubated for 5 minutes on ice. The sonication and incubation steps were repeated 5 times. Protein extraction from *E. coli* was done under native

conditions, using centrifugation of 12000 g for 30 minutes which clears the extract of inclusion bodies. The supernatant containing the soluble protein was used for protein-protein interaction assays ([www.bdbioscience.com](http://www.bdbioscience.com)). GST-tagged proteins were loaded on glutathione resin columns, and three steps of washing were done to remove any aspecific protein binding to the resin. Elution of GST-tagged protein was performed by adding elution buffer to the column in 1 mL fractions.

### **2.2.16 Leaf protein extraction**

*N. tabacum* plants were transformed using *A. tumefaciens* carrying the vector pVKH18EN6, containing the coding region for YFP<sub>Sec24</sub>. Leaves were infiltrated as described in section 2.2.14. Two entire leaves per construct were used (1 leaf = ~1.5-2g, ~60-70 cm<sup>2</sup>). Transformed plants were then placed in a growth chamber for 2 days. The expression of fluorescent protein was checked at the confocal microscope before proceeding with the extraction, not earlier than 48 hours after the plant transformation. Once the protein expression was confirmed, the transformed leaves were cut from the plant. To grind the transformed leaves, the leaf was split in half, cutting away the middle vein and the two halves of the leaf were placed into a mortar. Liquid nitrogen was poured on the leaves to snap freeze them and a pestle was used to create a fine powder. The powder was then transferred to a 15 mL Falcon tube, with 2.5 mL NE buffer per gram of leaves and protease inhibitor (Sigma P9599) at 33 µL/g of leaves. The mixture was incubated on ice until defrosted. At this point, the tube was mixed by vortexing and centrifuged at 4000 g for 10 minutes. The supernatant containing the protein leaf extract was filtered using



a membrane (Nitex filters 160 µm mesh), divided into Eppendorf tubes and centrifuged again at 14000 g for 15 minutes at 4 °C to pellet any remaining trace of debris. The clarified supernatants were collected into a single tube to have a homogeneous mixture, and used for interaction assays.

### **2.2.17 In vitro protein interaction: Histidine-pull down**

The coding regions for Sec22 and Sed5 were subcloned into the expression vector pET-28b (+) which contains a region coding for 6 histidines (His) at the end of the polylinker. The presence of the 6 His in the polylinker results in the addition of His to the C-terminus of the cDNA of the protein of interest inserted in the vector.

The His-tagged cDNA clones were used to transform the *E.coli* strain for protein expression in BL21. A single colony was initially inoculated into 5 mL of LB containing kanamycin (100 µg/mL) and incubated with agitation at 180 rpm for 15 hours at 37 °C. Successive steps were performed as described in 2.2.15.

Bacteria cells were resuspended in 1X equilibration buffer (1 mL/10 mL *E. coli* culture) ([www.bdbioscience.com](http://www.bdbioscience.com)). Cells were disrupted by sonication, and centrifuged at 12000 g for 30 min. The soluble supernatants were used for protein quantification by using a Coomassie (Bradford) protein assay kit based on the Bradford dye-binding procedure (Bradford, 1976). For protein-protein interaction assays, His-tagged protein extracts from *E. coli* were loaded onto Talon Metal affinity resin columns (2 mL) (BD Biosciences) for binding His-tagged proteins.

After three steps of washing to remove the aspecifically bound protein, the columns were loaded with 3 mL of the leaf protein extract expressing YFPsec24, and incubated by a gentle rotation for 1 hour at 4 °C. Successively, beads were pelleted with a centrifugation of 700 g for 5 minutes at 4 °C, and washed three times with wash buffer. Proteins bound to the beads were then eluted with elution buffer. Samples were diluted in 5x SDS-PAGE in a ratio of sample: buffer = 1:0.4 and were boiled for 5 minutes at 100 °C and loaded on a 10 % SDS-PAGE gel (section 2.2.18).

### **2.2.18 SDS-PAGE**

According to the method described by Laemmli (1970), proteins were separated by SDS-gel electrophoresis, and gels were set up as explained in the Appendix, (Table A8); the SDS-PAGE unit Mini-PROTEAN 3 electrophoresis cell from Bio-Rad was assembled, following the instructions in the Bio-Rad manual ([www.biorad.com](http://www.biorad.com)). Once prepared, the separating gel mix (Appendix, Table A8) was poured in the unit avoiding bubbles that might interfere with gel polymerization. The gel mix was then immediately covered with water saturated with butanol. Under these conditions, the gel polymerization happened within about 30 minutes. The butanol was discarded and the gel top surface was rinsed with distilled water. This step was followed by the preparation of the stacking gel (Table A8) that was poured on top of the separating gel after the insertion of the gel comb. Once the separating gel polymerized (about 30 minutes), the comb was removed and the wells were rinsed with distilled water. The module was assembled in a tank

filled with running buffer 1x. Protein samples were denatured by the addition of 5x sample buffer and heating at 95 °C for 5 minutes. Denatured samples were loaded on the gel by using a Hamilton syringe. The prestained protein marker was purchased from Fermentas (#SM0441) ([www.fermentas.com](http://www.fermentas.com)). The electrophoretic run was set at 100 V for 1-2 hours using a powerpac with an output of 250 V, 3.0 A, 300 W ([www.vwr.com](http://www.vwr.com)).

### **2.2.19 Western blotting**

After separation by SDS gel-electrophoresis, proteins were transferred by western blotting using a Bio-Rad mini PROTEAN3 trans-blot module (as described in [www.bio-rad.com/LifeScience/pdf/Bulletin\\_2895.pdf](http://www.bio-rad.com/LifeScience/pdf/Bulletin_2895.pdf)), to a nitrocellulose membrane (Life Sciences BIOTRACE NT 3M) ([www.vwr.com](http://www.vwr.com)). The transfer was done by using 1x blotting buffer for 60 minutes with a voltage of 100 V. At the end of the transfer, the membrane was rinsed in distilled water. Transferred proteins were visualized by the addition of Ponceau solution 0.1% for 30 seconds. The membrane was then washed with PBS-Tween 0.1 % with gentle agitation for 15 minutes, and with PBS for 5 minutes. This was followed by incubation with the blocking solution for a minimum of 4 hours to overnight. The nitrocellulose was then rinsed with PBS for 5 minutes twice, and incubated with a primary polyclonal antibody (rabbit) (antiGFP or antiGST or antiHIS diluted as described in section 2.1.4 in working solution as specified in the Appendix, Table A2) for a minimum of four hours at room temperature. Three 10 minute washing steps were performed with PBS-Tween, followed by incubation with the secondary antibody (goat anti-

rabbit IgG linked to horseradish peroxidase) (Santa Cruz Biotechnology, [www.scbt.com](http://www.scbt.com)). The secondary antibody was added at a dilution of 1:5000 in working solution (Appendix, Table A2) and incubated between 1 and 2 hours. Three washes of 10 minutes each in PBS-Tween were performed, followed by two 5 minute washes in PBS. This step was followed by incubating the blot with the enhanced chemiluminescence (ECL) solution (prepared as described in Table A2) for 1 minute. A GelDoc system was used to detect the chemiluminescence signal.

#### **2.2.20 Confocal microscopy**

Confocal microscopy, compared with optical and fluorescence microscopy, presents several advantages. In fact, it allows the observation of a select layer of a sample with a good resolution. The laser of the confocal microscope emits light that is reflected by a beam splitter, and that passes through an objective that focuses this light on the sample. This light excites the fluorescent protein expressed in the sample, and once excited, the protein releases light that is collected through the objective and directed in focus on the confocal pinhole. This light path allows out of focus light to be discarded and minimizes the out of focus signal that affects imaging from non-confocal fluorescence microscopes. Light emitted by the sample is collected by a photomultiplier. In addition, the presence of the beam splitter allows us to observe samples expressing proteins of different colors in the same confocal plane and at the same time, because it splits fluorescent emission accumulated by diverse photomultipliers (for further details [www.zeiss.com](http://www.zeiss.com)).

All the microscopy experiments were done 48 hours after leaf infiltration (as described in section 2.2.14) using a laser scanning confocal microscope ZEISS LSM510 META.

Roughly 1 cm<sup>2</sup> of leaf tissue was mounted in water on a slide for confocal images of tobacco leaf epidermal cells after *A. tumefaciens* infiltration. The 63x water immersion objective was used for analysis. Samples were analyzed at room temperature.

The argon ion laser at 488 nm was used for the excitation of green fluorescent protein (GFP) constructs, while the same laser at 514 nm was used for yellow fluorescent protein (YFP) constructs; the two proteins can be detected at the same time with the presence of the multitrack capabilities of the microscope. Different dichroic beam splitters and filters were used for GFP and YFP. The signals from the two fluorophores were detected using a 515-nm dichroic beam splitter and a 475-525 nm bypass filter for GFP, 515-nm dichroic filter and a 535- 590 nm bypass filter for the YFP, respectively. In this way, the problem of fluorescence cross-talk was avoided (Brandizzi et al., 2002a). To detect cyan fluorescent protein (CFP), a violet diode laser (405nm) was used. The emission signal from CFP was detected by a 460 nm dichroic beam splitter. The image size used in all the experiment was 512 x 512 pixel using the maximum scan speed. The laser intensity for these fluorescent proteins was respectively between 2 and 5 % for YFP, 10-25 % for GFP and 15-25% for CFP. The pinhole used for the different channels was 3 µm. The detector gain was set between 700 and 800. Zoom 3 was used to capture images and zoom 4 to observe details of cells. The line averaging used was 16 for still images and 8 for

time series to avoid bleaching of the sample. Imaging settings on the microscope, such as laser intensity, pinhole, detector gains, zoom and line averaging, were kept constant among different experiments with the same construct, to maintain similar experimental conditions. PaintShop Pro7 imaging suite was used for handling plus presentation of images.

#### **2.2.21 Brefeldin A (BFA) treatment**

A square piece (about 2 cm x 2 cm) of the transformed leaf was cut with a razor blade 48 hours after transformation and put in an Eppendorf tube containing brefeldin A (BFA) (Sigma B7651) at a concentration of 100 µg/mL for 1 hour, in the dark. The sample was then poured on a microscope slide and observed with the confocal microscope.

#### **2.2.22 BFA wash-out**

The sample used for the observation was carefully removed from the slide and poured in a beaker containing fresh tap water. The leaf sample was transferred to another beaker with new fresh water. The same operation was repeated three or four times. After that, the leaf sample was left overnight in an Eppendorf tube containing fresh water. The sample was subsequently poured on a slide and observed at the confocal microscope.

### 3. Results

#### 3.1 Sec24 subcellular localization

The first objective of this work was to establish the subcellular localization of (*A. thaliana*) Sec24 in plants. The fluorescent proteins GFP or YFP (G/YFP) were fused to the Sec24 N-terminus (G/YFPSec24) to preserve the function of the C-terminus in coat assembly (Stephens et al., 2000). G/YFPSec24 was expressed transiently or stably in tobacco leaf epidermal cells. In both cases, a diffuse fluorescence was detected in the cytoplasm and at punctate structures. To test whether Sec24 was localized at the peri-Golgi area, YFPSec24 was coexpressed with the *A. thaliana* K/HDEL receptor fusion ERD2GFP, a known ER/Golgi marker (Boevink et al., 1998; Brandizzi et al., 2002b; Saint-Jore et al., 2002). Co-expression of these two proteins showed a perfect localization of YFPSec24 at the peri-Golgi area (Figure 3.1 panel A, B and C). These data show that YFPSec24 is localized at the ERES (daSilva et al., 2004). To determine whether YFPSec24 structures and Golgi bodies were in continuous association, a time lapse experiment of cells co-expressing ERD2GFP and YFPSec24 was performed. As shown in Fig 3.1, Golgi stacks labelled by ERD2GFP tracked together with the ERES labelled by YFPSec24 (Figure 3.1 panels D, E and F).

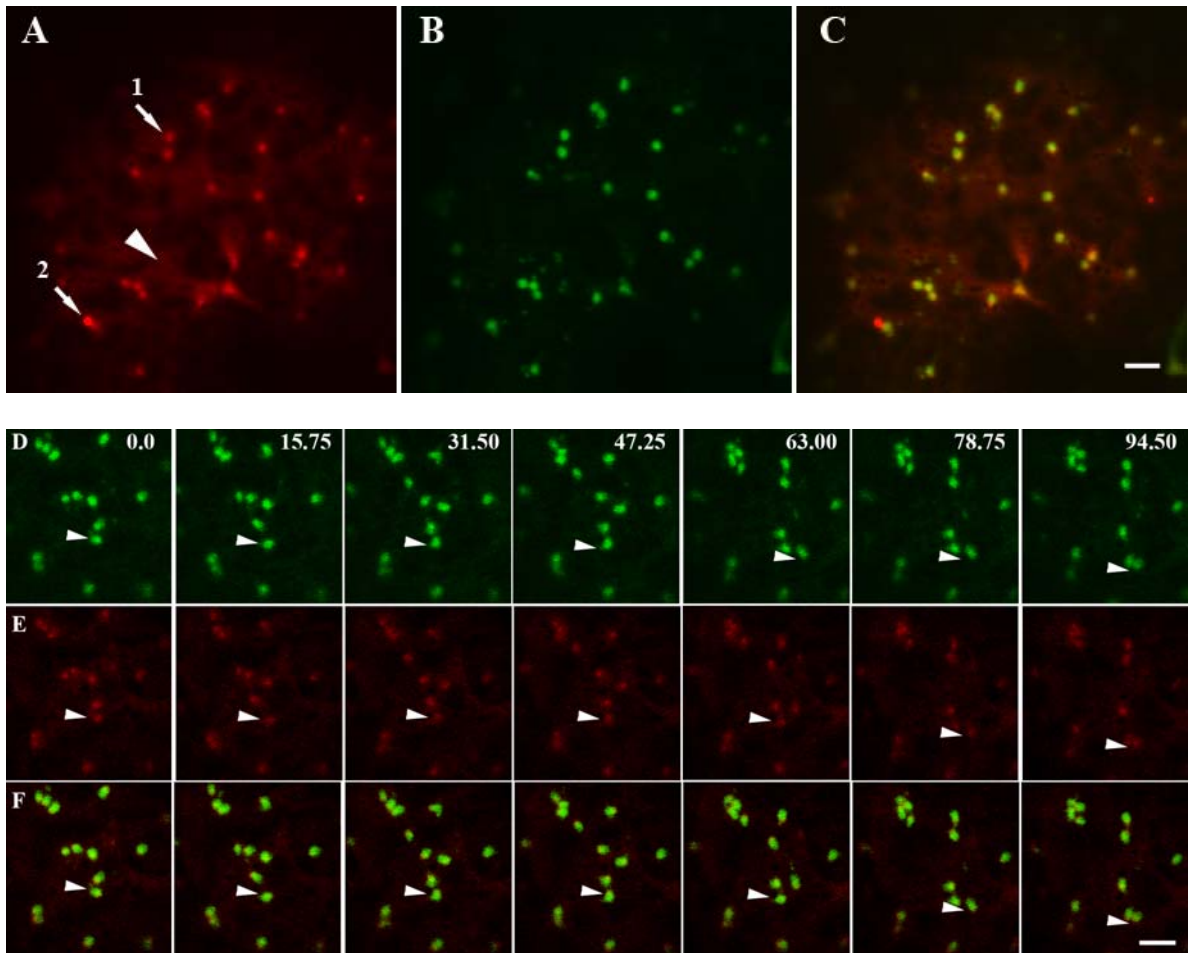


**Figure 3.1 ER export sites (ERES) and Golgi apparatus form secretory units.**

Confocal scanning images of YFPSec24wt (A), coexpressed with ERD2GFP (B), in transient expression 48 hours after leaf infiltration. YFPSec24 localizes at punctate structures (arrow 1) in the cytosol (arrowhead). The cytosol is represented as diffused fluorescence which surround black areas corresponding to tonoplast portions. As shown in the merged image (C), YFPSec24 was localized mostly at the peri-Golgi area, with the exception of rare extra punctate structures (arrow 2). Scale bar = 5  $\mu\text{m}$ . (D-F) Time lapse of a cell coexpressing YFPSec24 and ERD2GFP. Showing ERD2GFP (D), YFPSec24 (E), and merged image of D and E (F). Time (sec) of frame acquisition is indicated at the top of right corner. The arrowheads indicate mobile Golgi bodies that are continually attached to the YFPSec24 punctate structures during their movement. Scale bars= 5 $\mu\text{m}$



### **3.2 YFPsec24 retains functionality and interacts with Sec23.**

A fluorescent protein usually does not influence the biological activity of the protein with which it is fused (Miyawaki et al., 1997; Presley et al., 1997; Subramanian and Meyer, 1997; Tsien, 1998; Brandizzi et al., 2004). However, since the functionality of YFPsec24 protein fusion had never been tested before, we could not exclude that the prepared fusion could generate a mis-folded protein. Therefore to understand whether the fluorescent protein fusion YFPsec24 preserved its functionality, I checked its ability to interact with Sec23 to form a heterodimeric complex (Antonny and Schekman, 2001). I developed a glutathione-agarose affinity chromatography assay based on the interaction between a recombinant GSTSec23 and YFPsec24 expressed and extracted from plant leaves (Figure 3.2). Bound proteins were eluted and analysed by Western blot probed with an anti-GFP serum. Western blot analysis showed that YFPsec24 interacts specifically with GSTSec23 (Figure 3.2 line 5). These data not only indicated that Sec24 interacts with Sec23, as shown in mammalian cells (Stephens et al., 2000), but also that our YFPsec24 construct is a functional marker.

Once the protein's biological activity was verified, the next step focused on understanding how ERES activity and formation are regulated.

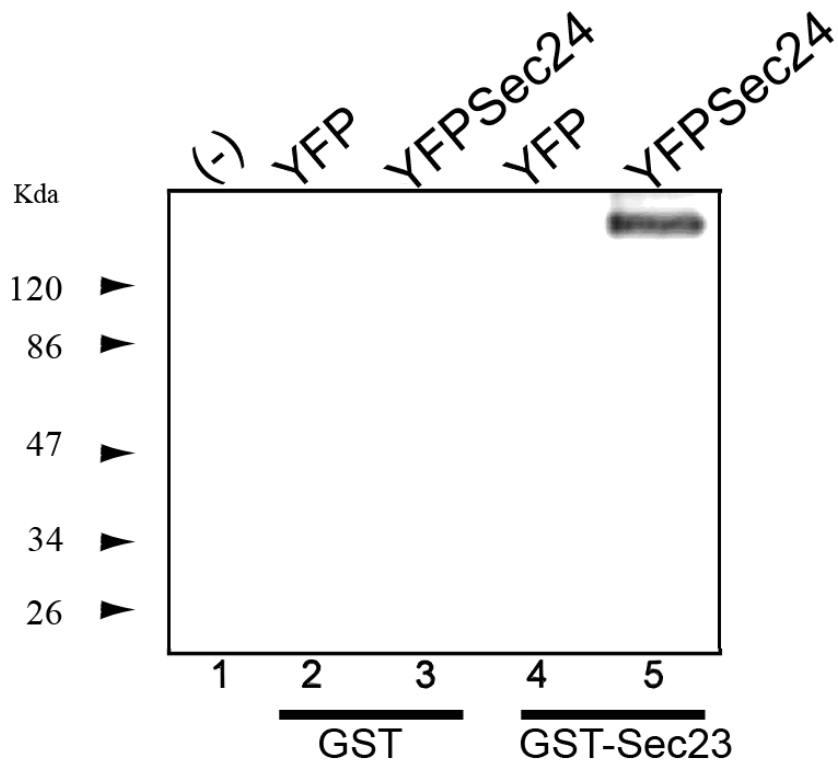


**Figure 3.2: The functionality of YFPSec24 is confirmed by interaction with the COPII component Sec23. Lanes 1-5:** Western blot probed with anti-GFP serum. Wild-type GSTSec23 (**lane 4 and 5**) was loaded on GST agarose beads and incubated respectively with cytosolic YFP (**lane 4**); or with YFPSec24 plant extract (**lane 5**). YFPSec24 has predicted molecular mass of 141 Kda. YFP was used as a negative control to exclude non specific interactions of YFP with GST agarose beads. Cytosolic YFP has a predicted molecular mass of 27 Kda. Negative control (**lanes 2 and 3**): YFP and YFPSec24 were loaded on empty GST beads and loaded on the GST column to exclude non specific interactions of these proteins with the resin. Negative control (**lane 1**): purified GST was loaded on beads incubated with YFPSec24, to exclude nonspecific interactions of YFPSec24 with GST. On the left of the western blot is the pre-stained protein molecular weight marker. This picture has been published (Stefano et al., 2006).

### **3.3 ERES stability is influenced by the anterograde pathway**

The next aim was to investigate the regulation of ERES identity in plants. First, I was interested in what would happen to ERES in the absence of active forward protein export from the ER. To check this, a mutant of Sar1 protein, Sar1H74L, which is locked in the GTP form, was used (daSilva et al., 2004). This mutant shows a slower GTP turnover in comparison to wild type Sar1 (Aridor et al., 1995). Overexpression of this mutant is known to disrupt ER export in yeast, mammals, and plants (Kuge et al., 1994; Shima et al., 1998; Zaal et al., 1999; Andreeva et al., 2000; Takeuchi et al., 2000; Phillipson et al., 2001; Ward et al., 2001; daSilva et al., 2004). In plant cells this mutant protein is localized in the cytosol and at punctate structures in conditions of low expression; however, a cytosolic distribution has been observed in cells overexpressing the mutant (daSilva et al., 2004).

To investigate ERES stability in the absence of cargo export from the ER, GFP<sub>Sec24</sub>wt was co-expressed with the Sar1 mutant Sar1 (H74L). Under these conditions, a pronounced cytosolic labelling of GFP<sub>Sec24</sub> was observed. In addition, the localization of this protein at the peri-Golgi area had disappeared (Figure 3.3). Therefore, under conditions of disruption of anterograde transport between the ER and the Golgi, Sec24 is no longer recruited to ERES. This confirms that ERES exist by virtue of cargo secretion.

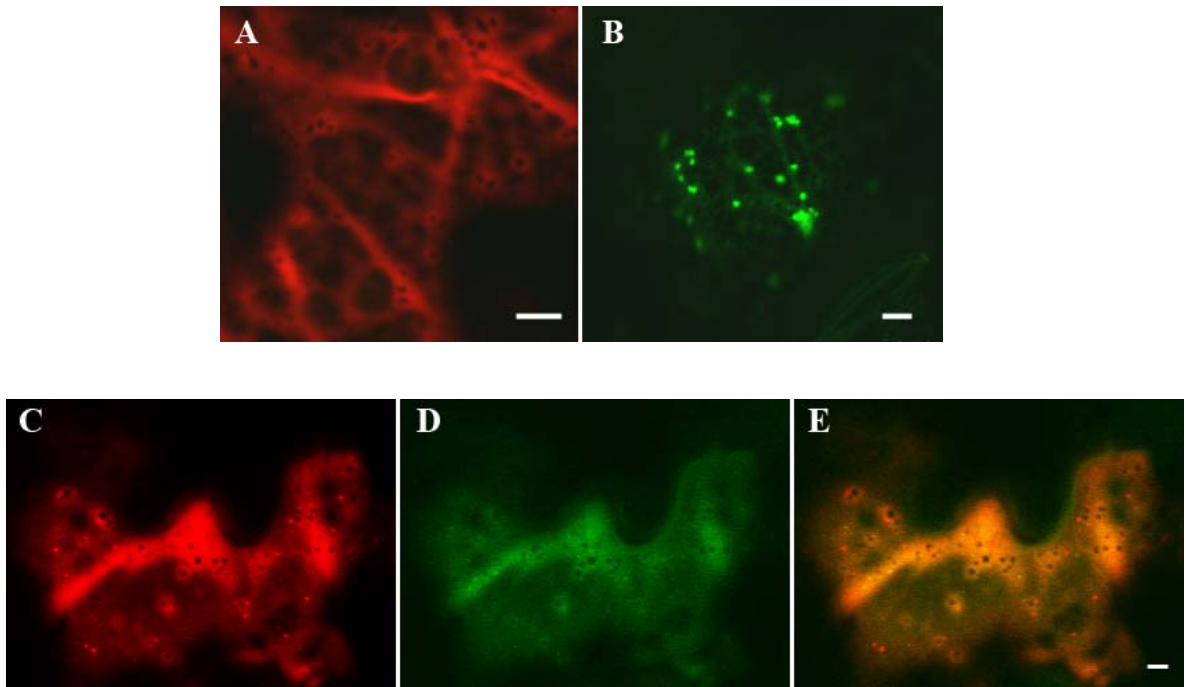


**Figure 3.3: Arrest of the anterograde pathway by the GTP mutant of Sar1 hampers the stability of the ERES.** Images show cells over-expressing Sar1GTPYFP alone (A) or GFPSec24wt alone (B). In cells co-expressing Sar1GTPYFP (C) and GFPSec24wt (D) localization of Sec24 at the peri-Golgi area disappears. Sar1GTPYFP is distributed in the cytosol and at punctate structures, as confirmed by daSilva et al. (2004), GFPSec24wt is distributed only in the cytosol as shown in the merged image (E). Scale bars = 5  $\mu$ m.

### **3.4 Retrograde pathway inhibition compromises ERES stability**

#### **3.4.1 Disruption of the retrograde pathway by Arf1 mutants**

Having established the influence of the integrity of the anterograde pathway on the localization of Sec24, I next wanted to analyze the influence of the retrograde pathway on the integrity of ERES. To do this, I needed to disrupt the COPI machinery by down-regulating the activity of Arf1. I used the mutated form of Arf1 that is blocked in the GDP form through a point mutation of a conserved Threonine (T31N) (Teal et al., 1994). The mutant blocked in the GDP form is cytosolic and unable to bind the Golgi membrane (Stefano et al., 2006). Therefore, Arf1GDP is not able to form COPI vesicles (Xu and Scheres, 2005). I also used the mutated Arf1 blocked in the GTP form (mutation Q71L), which is able to initiate COPI assembly, and allow slow release of the COPI coat (Stefano et al., 2006). This results in reduced activity in protein transport from the Golgi to the ER.

When a GFP fusion of Arf1GTP (Arf1GTPGFP) is expressed at low levels, it is localized at punctate structures, including the Golgi apparatus, while under conditions of overexpression, it assumes a cytosolic distribution (Stefano et al., 2006). The use of these mutants gives us the tools to understand whether a compromised COPI activity has any negative influence on the ER export machinery.

Wild type Arf1-GFP is localized at the Golgi and extra punctate structures that bud from the Golgi apparatus (Stefano et al., 2006). Coexpression of YFPsec24 with wt Arf1GFP did not affect the distribution of Sec24 at the ERES (Figure 3.4). When YFPsec24 was coexpressed with the mutant Arf1GDPGFP, YFPsec24 was redistributed completely to the cytosol (Figure 3.5).

Coexpression of YFPsec24 with Arf1GTPGFP gave different phenotypes: cells expressing Arf1GTPGFP at low levels showed YFPsec24 and the Arf1GTPGFP on punctate structures ( Figure 3.6 A, B and C); while cells overexpressing Arf1GTPGFP both Arf1 mutant and YFPsec24 were redistributed to the cytosol (Figure 3.6 E, F and G).

These results suggest that when the machinery for protein transport from the Golgi to the ER is disrupted, the delivery of membrane proteins to the Golgi and the integrity of ERES are compromised.

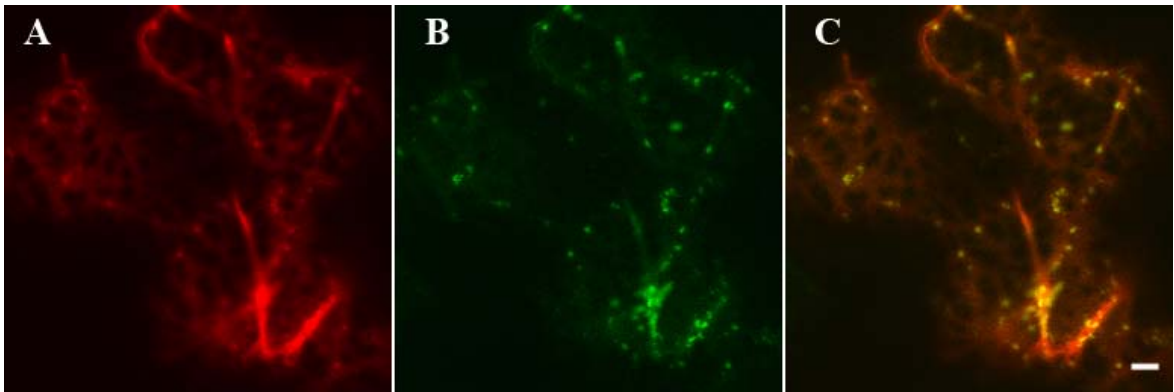


**Figure 3.4: Arf1GFPwt does not affect the localization of YFPsec24.** YFPsec24 (A) coexpressed with Arf1GFPwt (B); (C) = A and B merged. Scale bar = 5  $\mu$ m.

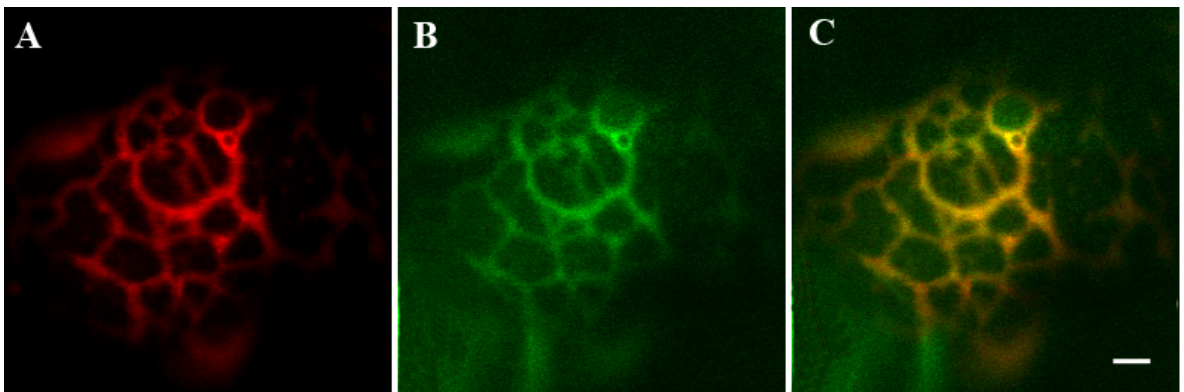


**Figure 3.5: Inhibition of the retrograde pathway by the Arf1 mutant blocked in the GDP form compromises ERES stability.** YFPsec24 (A) coexpressed with Arf1GDPGFP (B). In the presence of the GDP mutant, the localization of YFPsec24 at ERES disappears and the YFP fluorescence is distributed in the cytosol (C). Scale bar = 5  $\mu$ m.

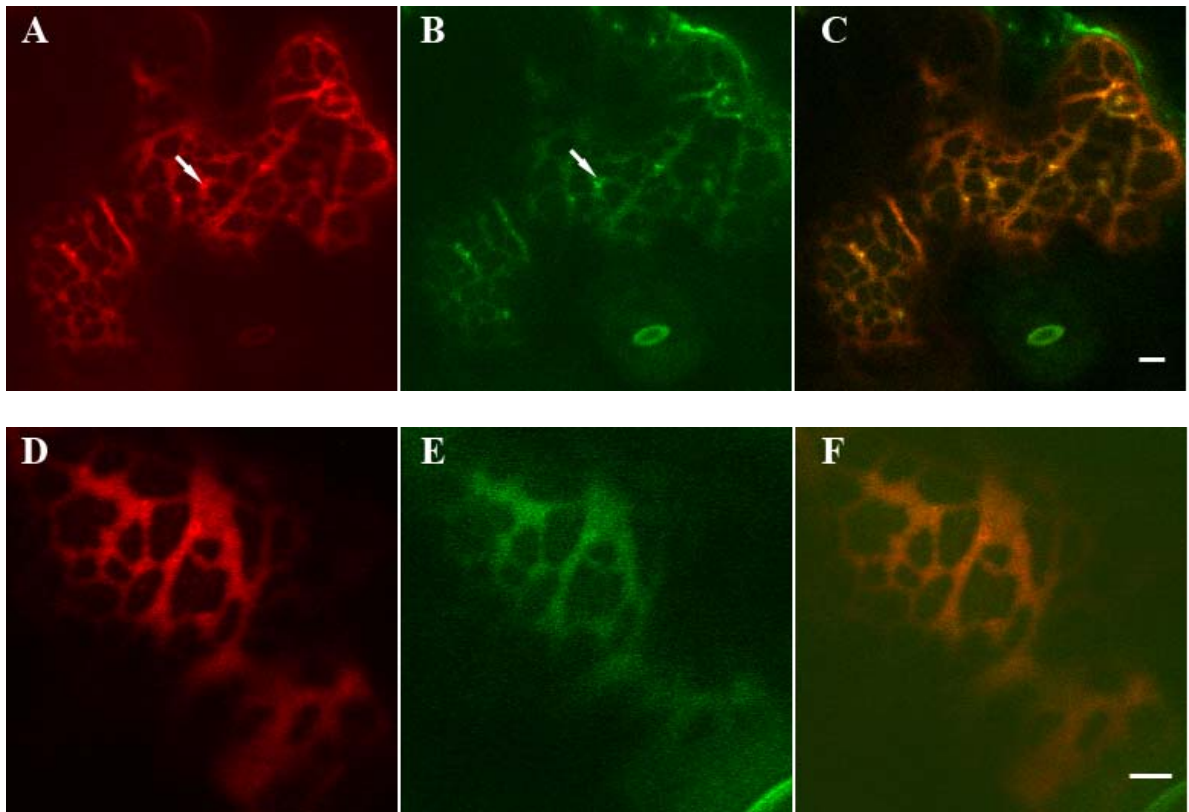


**Figure 3.6: Overexpression of the Arf1 mutant blocked in the GTP form compromises the ERES stability.** YFPsec24 (A and D) coexpressed with Arf1GTPGFP (B and E). Under condition of low Arf1GTPGFP expression, Arf1GTPGFP (B) and YFPsec24 (A) localize on punctate structures. Under conditions of Arf1GTPGFP overexpression, the localization of YFPsec24 (D) is only in the cytosol, as was also shown in the presence of the GDP mutant (C). Scale bar = 5  $\mu$ m.



### 3.4.2 Chemical inhibition

To gain further insights into the inhibitory effect of retrograde transport on ER protein export, a pharmacological agent was also used. The rationale behind this choice was that coexpression analyses are based on simultaneous expression of YFP<sub>Sec24</sub> and Arf1 mutants. Therefore, this approach does not allow us to distinguish whether Arf1 mutants prevent Sec24 binding to ERES or if they disrupt the binding of Sec24 already attached to ERES. The use of pharmacological agents on cells expressing GFP<sub>Sec24</sub> at 2 days after transformation can instead allow us to distinguish these two possibilities. The fungal metabolite brefeldin-A (BFA) is an inhibitor of Arf1GEFs (Donaldson et al., 1992b; Helms and Rothman, 1992; Zeeh et al., 2006). When BFA is added to the cells, the immediate effect is the relocation of Arf1 to a cytosolic pattern (Donaldson et al., 1991; Vasudevan et al., 1998; Takeuchi et al., 2002). Furthermore, upon addition of the drug, the Golgi is quickly disorganized, and its membranes are redistributed to the ER (Donaldson et al., 1992a; Helms and Rothman, 1992). Therefore this drug was used to understand whether the GFP<sub>Sec24</sub> localization at the peri-Golgi area depends on the active process of secretion and corresponds to an active equilibrium between recruitment and dissociation of Sec24. Segments of leaves coexpressing YFP<sub>Sec24</sub> and ERD2GFP were therefore treated with BFA and the distribution of these markers with a confocal microscope was followed. Under these conditions, ERD2YFP was relocated to the ER and GFP<sub>Sec24</sub> was no longer recruited to the peri-Golgi area (Figure 3.7, panel D,E,and F).

To test whether this effect was reversible, BFA was washed-out. GFPSec24 was observed to accumulate near a reformed Golgi body (Figure 3.8).

These data demonstrated that inhibition of retrograde protein transport affects the integrity of ERES most likely preventing Sec24 from binding to ERES.

Furthermore, these data support a model whereby Golgi integrity is linked to ERES function.

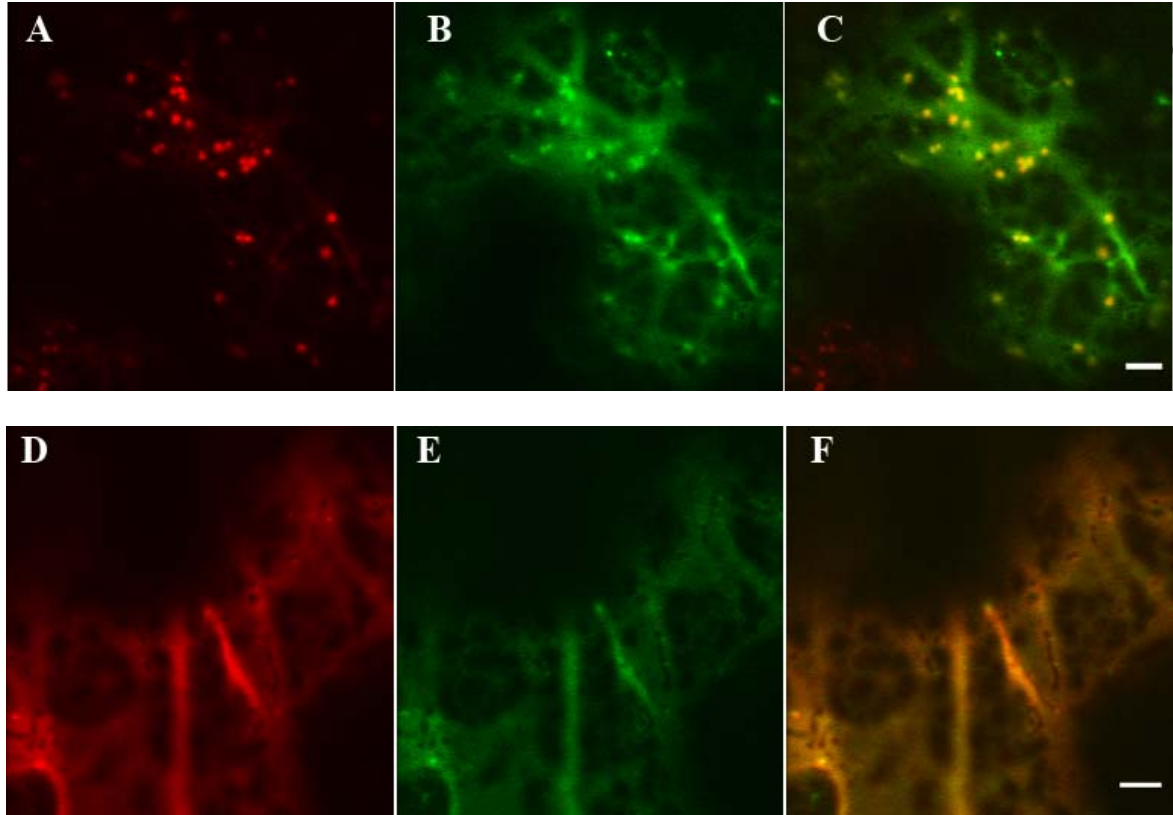


**Figure 3.7: Chemical inhibition of the COPI pathway causes a block in ERES formation.** Panels A, B and C show the localization of GFPSec24, ERD2YFP and their merged localization before the treatment with BFA, respectively. Panels D, E and F show GFPSec24, ERD2YFP, and their merged localization after 1 hour of incubation in BFA. The effect of BFA on COPI vesicle formation through a direct action on Arf1, influences the localization of the Golgi marker ERD2GFP, which is completely localized in the ER. The COPII component Sec24 is redistributed to the cytosol in presence of BFA. Scale bars = 5  $\mu$ m.

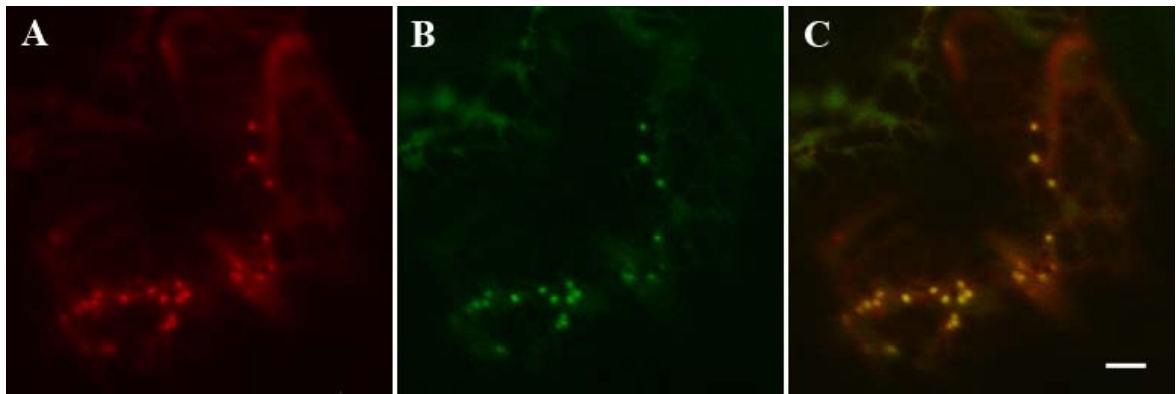


**Figure 3.8: The chemical block caused by the BFA is completely reversible upon wash-out.** GFPSec24 (A), coexpressed with ERD2YFP (B), after recovery from BFA treatment. Both fluorescent protein fusions of Sec24 and ERD2 relocate at the peri-Golgi area after removal of the drug (C). Scale bar = 5  $\mu$ m.

### **3.5 Biochemical support for the interaction of Sec24 with SNAREs:**

#### **Histidine pull-down for protein interaction between Sec24-Sed5 and Sec24-Sec22**

At the site of vesicle formation, the Sec23/24 complex collaborates in order to recruit v-SNAREs at the level of ERES formation (Kuehn et al., 1998). It is then probable that the purpose of the binding between Sec24 and Sed5 is to help in the process of cargo selection (Peng et al., 1999; Miller et al., 2005). As this aspect of the function of Sec24 is still unexplored in plants, protein-protein interaction experiment using a histidine-agarose affinity chromatographic assay was carried out. The construct YFPSec24 and cytosolic YFP (cYFP) were used to transform leaves, followed by a protein extraction. The extract was passed through Nickel/Cobalt columns, in which Sed5His or Sec22His were previously immobilized. The YFP extract was used to demonstrate that the interaction was not due to the affinity of the SNARE protein with the YFP. Bound proteins were eluted and analyzed by Western blot with antiGFP serum. The result shows a specific interaction between Sec24 and the SNAREs Sed5 and Sec22 (Figure 3.9, lines 3 and 2).

This result is important because it represents, for the first time in plants, that Sec24 interacts specifically with SNAREs.

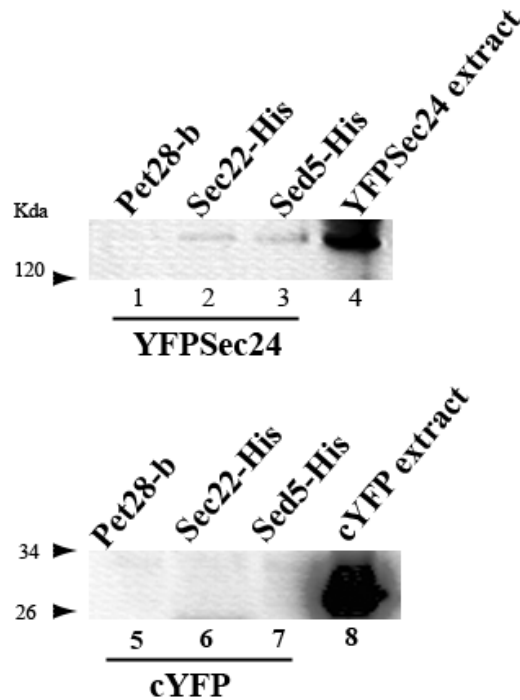


**Figure 3.9: The Histidine-pull down demonstrates an interaction between wt Sec24 with Sed5 and Sec22. Lanes 1-4:** Western blot probed with anti-GFP serum. Two SNARE proteins: Sec22His (**lane 2**) and Sed5His (**lane 3**), extracted from *E.coli*, were loaded on nickel/cobalt column and incubated with YFPSec24 extracted from leaves. **Lane 1:** shows the negative control in which the 6xHistidine tag expressed by the empty vector (pET28b) was loaded on the column and incubated with Sec24, under the same experimental conditions as the two SNAREs. **Lane 4:** shows a positive signal for the YFPSec24 extract. YFPSec24 has predicted molecular mass of 141 Kda. **Lanes 5-8:** negative controls show that the interaction is specific. **Lane 5:** represents the negative control, where the 6xHistidine tag expressed by the empty vector (pET28b) was incubated with cYFP. Cytosolic YFP has a predicted molecular mass of 27 Kda. No YFP interaction with the the His-tag was detected, indicating that the tag of with YFP is not responsible for an interaction of YFPSec24 with SNAREs. Sec22His (**lane 6**) and Sed5His (**lane 7**) were loaded on Nickel/ Cobalt column and then incubated with cYFP. No interaction was detected, thereby excluding the possibility that the YFP tag of Sec24 was responsible for the interaction with SNAREs. **Lane 8:** is the leaf protein extract of cYFP, showing the specificity of the serum.

### **3.6 Identification of important residues for the interaction between Sec24 and SNAREs**

Once the interaction between Sec24-Sed5/Sec22 was established, the next step was to understand the role of this interaction and whether this interaction could be important for Sec24 to select cargo. To do so, crystallographic analyses on yeast Sec24 were used to identify conserved surface domains of this protein within plant Sec24 that may be important for Sec24's interaction with SNAREs (Bi et al., 2002). In particular it has been suggested that certain Sec24 hydrophobic residues may be potential binding sites for SNAREs (Bi et al., 2002). These are Tyrosine 296, Valine 557, and Leucine 616. Therefore a sequence alignment of the yeast Sec24 and *A. thaliana* Sec24 were performed using ClustalW. This would allow us to find the corresponding residues putatively involved in an interaction between plant Sec24 and the SNAREs.

The result of the alignment suggested that all the three amino acids corresponding to Tyr438, Val689, and Leu749 were conserved (Figure 3.10).

```

Arabidopsis thaliana      401 DVPGEYFSLHDATGRMDMDQRPELTKGSVEIIAPTEY MVRPPMPPIYFF 450
Saccharomyces cerevisiae 451 DVP-MQMDQSDPNDPKSRYD-RNEIKCAVMEYMAPKEY TLRQPPPATYCF 308
      ***   .:. *... :   * * *:. . : * : ** . ** : * * * . * *

```

```

Arabidopsis thaliana      643 IASLGTLAKYTGQVYYPGFQSSVHG--DKLRHELARDLTRETAWEA VM 690
Saccharomyces cerevisiae 509 VASLSNLSRFTAGQTHFYPGFSGKNPNDIVKFSTEFAKHISMDFC MET VM 558
      :***. . *::: * . ** : : ** * . . . . . * : * : * : : : . : * : *

```

```

Arabidopsis thaliana      741 TVYFQVAL Y TASCGERIRVHTSVAPVVTDLGEMRQADTGSIVSLYAR 790
Saccharomyces cerevisiae 608 YCYVQVAV L LSLNNSQRRIRIITLAMP TTESLAEVYASADQLAIASFYNS 657
      * . *** : * : . . : * * * : * . * . . . * . * : * * : * : * : *

```

**Figure 3.10: A high conservation in residues involved in protein-protein interaction was found between yeast and *Arabidopsis* Sec24.** ClustalW alignment of *Arabidopsis* Sec24 (AAM97042) with *Saccharomyces cerevisiae* (NP\_0121571). This alignment shows a conservation of amino acids Tyr296, Val557, and Leu616 in yeast Sec24. This corresponds to the *Arabidopsis* Sec24 residues: Tyr438, Val689, and Leu749.



### 3.7 Mutagenesis and subcellular localization of Sec24 mutants

The next step was to determine if mutation of these residues had an effect on the distribution of Sec24. I hypothesized that disruption of the binding of Sec24 to SNAREs would reduce the efficiency of recruitment of Sec24 onto ERES. Therefore, after the identification of the Sec24 conserved residues putatively involved in the interaction with SNAREs, three Sec24 mutants were generated by site-directed mutagenesis. I then fused their coding sequence to YFP, followed by subcloning the sequence into the pVKH18En6 expression vector. The resulting mutants were named YFPsec24Y438A, YFPsec24V689A, and YFPsec24L749A. Proteins were expressed in tobacco leaf epidermal cells by *Agrobacterium*-mediated infiltration. Laser confocal microscopy revealed that all of these mutants showed a more cytosolic localization when compared with the wild type (Figure 3.11). This indicated that these Sec24 mutations may be responsible for a decreased efficiency in Sec24 binding to the ERES.

To explore further these Sec24 mutants, I coexpressed each mutant with ERD2GFP. I hypothesized that the Sec24 mutants would be recruited to ERES in the presence of a large amount of membrane cargo in need of export from the ER if the interaction of the Sec24 mutants with SNAREs or ER export competent cargo was reduced but not abolished. Coexpression of the Sec24 mutants with ERD2GFP showed that the mutants were distributed at ERES (Figure 3.12-3.13-3.14). This result resembles the induction by Sar1 recruitment to ERES upon cargo overexpression (daSilva et al., 2004). This experiment suggests that the interaction of the Sec24 mutants with SNAREs and/or cargo is reduced but not abolished.

Unfortunately, due to lack of time, it was not possible to test whether this effect was specific to an interaction with SNAREs. This should be the focus of future studies to better characterize the relevance of the Sec24/SNAREs interaction to ER export in plants.

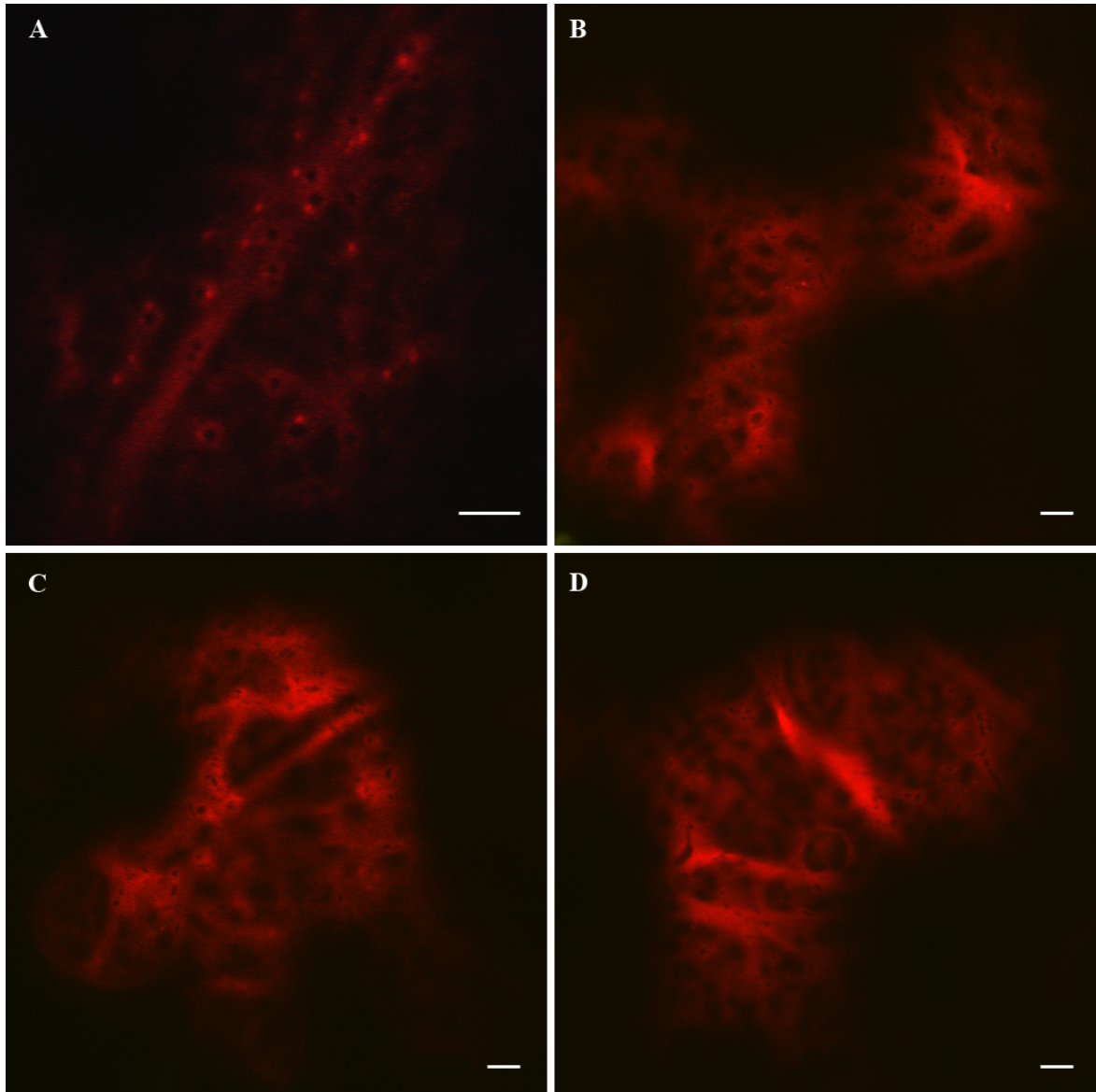


**Figure 3.11: The different subcellular localization between YFPSec24wt and YFPSec24 mutants suggest a reduced functionality of the mutated proteins compared to the wt.** Different localization of YFPSec24wt (A), YFPSec24Y438A (B), YFPSec24V689A (C), and YFPSec24L749A (D). It is possible to appreciate the difference in localization between Sec24wt and the mutants. While YFPSec24wt is present at ERES, the Sec24 mutants (B, C, and D) are predominantly cytosolic. Scale bars = 5  $\mu\text{m}$ .

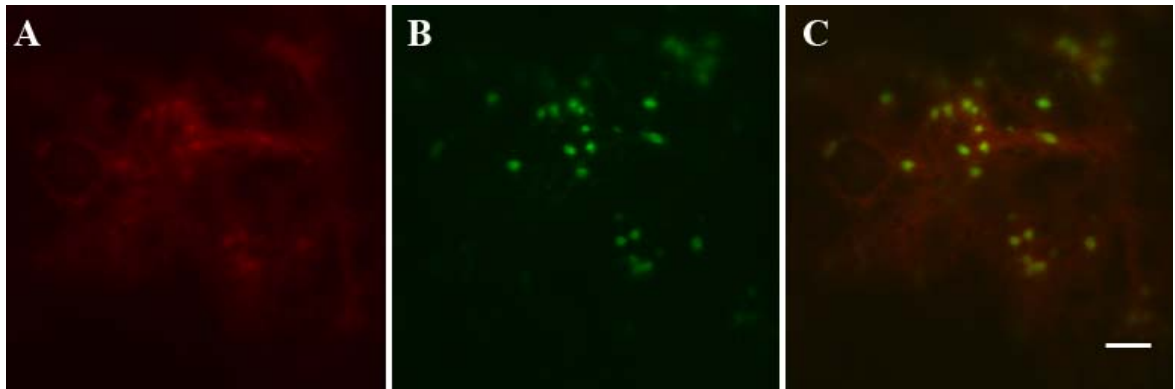


**Figure 3.12: In presence of cargo, the recruitment of the YFPSec24Y438A is increased.** YFPSec24Y438A (A) coexpressed with ERD2GFP (B). In the presence of a cargo protein, like ERD2, the mutant changes its localization and reappears at the level of the Golgi. Scale bar = 5  $\mu$ m.

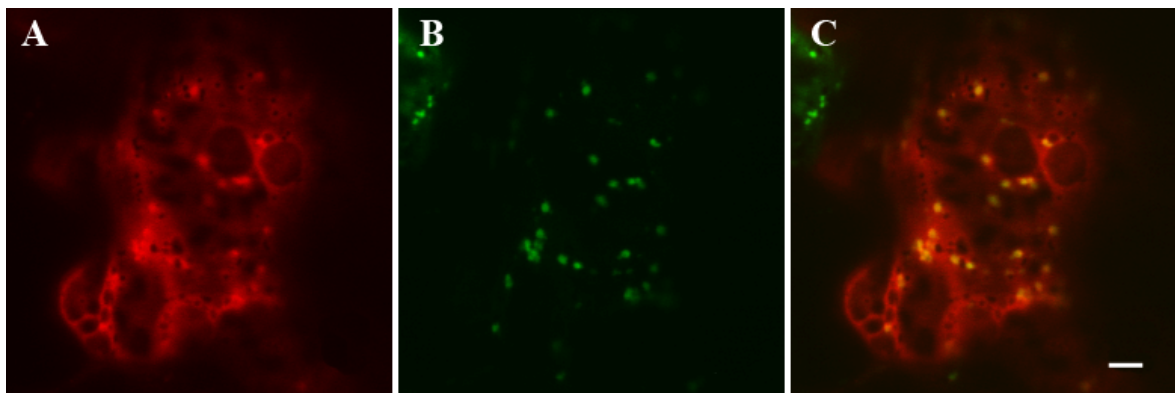


**Figure 3.13 In presence of cargo the recruitment of the YFPSec24V689A is increased.** YFPSec24V689A (A) coexpressed with ERD2GFP (B). In presence of cargo protein, like ERD2, the Sec24 mutant changes its localization and reappears at Golgi level. Scale bar = 5  $\mu$ m.

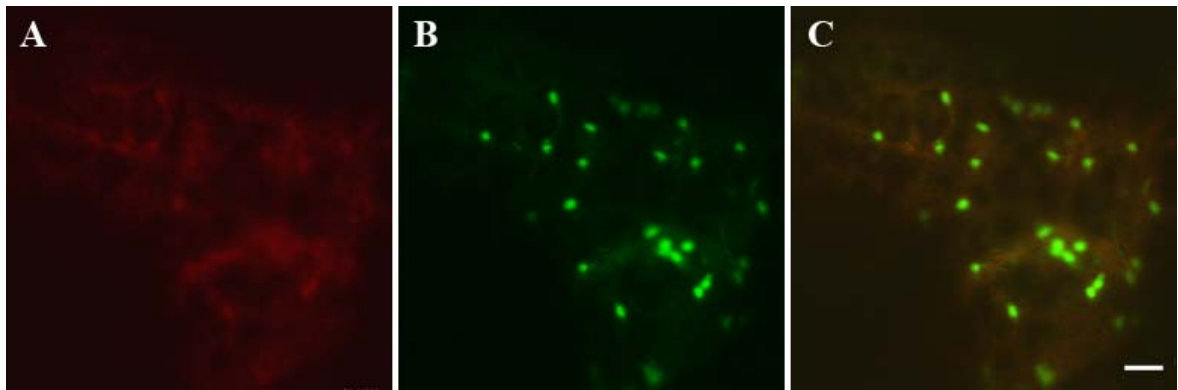


**Figure 3.14** In presence of cargo the recruitment of the YFPSec24L749A is increased. YFPSec24L749A (A) coexpressed with ERD2GFP (B). In the presence of cargo protein, like ERD2, the Sec24 mutant changes its localization and reappears at the peri-Golgi level. Scale bar = 5  $\mu$ m.

## **4. DISCUSSION**

### **4.1 ERES are distributed at the peri-Golgi area in *N. tabacum* epidermal leaf cells**

The mechanisms regulating the protein transport from the ER to the Golgi in plant cells are very interesting and a matter of recent investigation and debate (Hanton et al., 2006). To analyse the COPII mediated export from the ER, this study was conducted on one of the COPII coat structural components, Sec24. Previous work that focused on the dynamic of two COPII regulatory proteins, Sec12 and Sar1, demonstrated the first evidence of ERES existence in plant cells (daSilva et al., 2004). The data collected on Sec24 localization and its dynamics in this study confirmed that ERES are distributed at the peri-Golgi area (Figure 3.1). It was also found that the existence of rare additional bright structures do not co-localize at ERES (Figure 3.1). Similar structures were observed with a fluorescent fusion of Sar1 (daSilva et al., 2004). It could be hypothesized that these additional structures are developing ERES that may correspond to the early differentiation of new Golgi bodies.

Much controversy exists in the plant field about the dynamics of protein transport from the ER to the Golgi. In particular, it has not been conclusively established where ERES are distributed in plant cells. The observed association between the ERES marked by Sec24, and the Golgi marked by ERD2 during Golgi movement validates the secretory unit model (daSilva et al., 2004), as it supports that Golgi and ERES are tightly associated and move together on the ER surface. A

recent publication has indicated that punctate labelled with the COPII component Sec13 are not always associated with Golgi bodies (Yang et al., 2005). This observation has been made in BY2 cells, whereas in this study tobacco leaf epidermal cells were used. It is possible that different cell systems have different ERES distribution. Alternatively, it is possible that the Sec13 isoform used by Yang et al. (2005) associates preferentially with some ERES rather than others. This would be consistent with the large number of COPII protein isoforms that exists in plants (Andreeva et al., 1998; Andreeva et al., 2000).

daSilva et al. (2004) demonstrated that accumulation of Sar1 at ERES is enhanced in conditions of cargo molecule over-expression. Our data showed a localization of Sec24 at ERES in the absence of a high level of cargo expression. The accumulation of Sec24 at ERES in the absence of cargo over-expression could be due to the involvement of Sec24 in the process of cargo selection (Miller et al., 2002). In this view it is probable that a basal level of protein export from the ER is sufficient to ensure a distribution of Sec24 on ERES. Alternatively, the localization of Sec24 at ERES may be explained by differential dynamics of Sec24 and Sar1 at ERES that resemble the dynamics of the COPI components, Arf1 and coatamer in plant cells. By following the dynamic association and dissociation of Arf1 and coatamer from Golgi membranes by fluorescence recovery after photobleaching analysis (FRAP) it was found that Arf1GFP cycles faster than a fluorescent fusion of the COPI component  $\epsilon$ -COP (Stefano et al., 2006). It was then hypothesized that Arf1 cycles faster than coatamer on Golgi membranes to create a COPI domain on the Golgi (Matheson et al., 2006). We can hypothesize a similar difference in

kinetics of the COPII components Sar1 and Sec24. Sar1 may cycle on and off membranes faster than Sec24. If this were the case, Sar1 would be less detectable on membranes than Sec24. Therefore, an explanation for the different distribution of Sar1 and Sec24 on ERES may be attributable to differences in cycling kinetics of these two proteins.

#### **4.2 An equilibrium between anterograde and retrograde pathway is important for protein cycling at the ER/Golgi interface.**

This work demonstrates that ERES integrity depends on an active anterograde pathway (Figure 3.5, 3.6, 3.7). This was shown by expression of a Sar1 mutant blocked in a permanent status of activation in cells co-expressing the ERES marker Sec24. Loss of ERES integrity is most likely due to disruption of COPII vesicle budding induced by the Sar1 mutant.

Over-expression of the mutant Sar1GTP also caused inhibition of the anterograde pathway and consequent reabsorbance of the Golgi marker ERD2GFP into the ER (daSilva et al., 2004). The data provided by this study reinforce these results. The block of protein transport is most likely due to reduction of COPII vesicle formation at ERES consequent to Sar1 inactivity that primes COPII vesicle formation. Consequently, Golgi protein cargo is blocked in the ER and cannot be exported to the Golgi (daSilva et al., 2004). In the meantime, Golgi proteins cycle to the ER via the retrograde route. This results in redistribution of Golgi proteins in the ER.



The obtained data also indicate that retrograde protein transport from the Golgi to the ER is necessary to maintain the integrity of ERES and therefore the retrograde and anterograde pathways are related and balanced (Figures 3.5, 3.6 and 3.7). This was demonstrated by following the effects of a disruption of Arf1 activity. I found that Arf1GTP mutants binds Golgi membranes at a low level of expression and the cycling of Golgi enzymes between the ER and Golgi is reduced in comparison to a control (Stefano et al., 2006). Under these conditions, Sec24 was localized at ERES. However, when Arf1GTP was expressed at high levels, Golgi membranes collapsed into the ER and a cytosolic localization of both constructs: Arf1GTPGFP and YFPsec24 was observed. When the GDP mutant of Arf1 was expressed, the assembly of the COPI machinery at Golgi membranes was hampered and ERES integrity was compromised (Stefano et al., 2006).. Under these conditions, both proteins have a cytosolic localization. In agreement with daSilva et al. (2004), the data collected in this study showed that ERES integrity depends on the presence of intact, functional COPI machinery (Stefano et al., 2006). The result given by the combined expression of Arf1GDP and Sec24 is also reproducible with pharmacological agents. The addition of BFA, which inhibits the activation of Arf1 (Donaldson et al., 1992a; Helms and Rothman, 1992), blocks COPI machinery formation and induces ERES collapse.

The tight interdependence between COPII and COPI verified in our system is most likely due to the fact that proteins, such as SNAREs, that are involved in ER protein export, shuttle between the ER and Golgi via a recycling process. When the retrograde route is hampered, the forward route out of the ER collapses due to lack

of cycling of essential components that are necessary for COPII formation between the ER and Golgi. This means that ERES and Golgi structures are maintained by the sequential, combined and balanced activity of the Sar1-COPII and Arf1-coatamer systems, which allow their components to cycle through the ER. In absence of the combined activity of COPI and COPII, the traffic in and out the Golgi is blocked. Therefore, the retrograde pathway mediated by COPI is of crucial importance for the differentiation of the ERES formed by the Sar1-COPII system.

#### **4.3 The identification of an interaction between Sec24 and SNAREs could be the key to understanding the mechanism of protein export from the ER in plants**

It is yet unknown in plants whether the function of cargo selection is directly operated by Sec24, or whether it needs the contribution of an intermediate factor to activate or to expose specific Sec24 sites for particular cargo protein selection. The molecule that could act in this capacity may be SNARE proteins. SNAREs usually make contact with COPII components at the stage of the pre-budding complex, when only three (Sar1, Sec23 and Sec24) of all the components are present (Mancias and Goldberg, 2005; Miller et al., 2005; Sato and Nakano, 2005). The most common role of these proteins is to promote vesicle fusion, but recently it has been demonstrated that they have a more complex function than originally thought.

It has been shown that the t-SNARE Sed5 cycles between ER and Golgi (Wooding and Pelham, 1998). The pre-budding complex recruits v-SNAREs on the ERES, and the interaction between Sed5 and Sec24 can be explained by an

interaction between these two proteins during cargo selection (Peng et al., 1999; Miller et al., 2005).

Therefore, if SNAREs work as intermediate molecules for facilitating cargo selection, it would be interesting to determine whether Sec24 interacts with SNAREs in plants, and with which kind of SNAREs. It has been shown in yeast that Sec24 interacts with Sed5 (t-SNARE) and Sec22, a potential retrograde v-SNARE that can be exported from the ER in two forms: as a monomer or as part of the t-SNARE complex (Mossessova et al., 2003a). It has also been postulated that in the sequence of Sec24 there may be specific sites for interaction with either the cargo or a SNARE proteins (Bi et al., 2002). A crystallographic analysis provided a classification of different domains of Sec24 indicating the most probable candidates to be directly involved in protein-protein interaction (Bi et al., 2002). However, no experimental support to determine whether the identified domains were actually responsible for the postulated interaction has been produced. I hypothesized that by homology I could identify similar residues and test their relevance for a SNARE interaction with Sec24. When I mutated the conserved Sec24 residues for a putative Sec24/Sed5 interaction I found interesting results. The observation of a more cytosolic localization of the YFP fusions of the Sec24 mutants suggests that Sec24 mutants are not functioning properly as they do not bind ERES efficiently. However, coexpression of the Sec24 mutants with the Golgi marker ERD2 shows an obvious recruitment of Sec24 mutants onto ERES. This resembles Sar1 behaviour under conditions of cargo over-expression (daSilva et al., 2004). There are at least three possible explanations for the behaviour of the Sec24 mutants. One possibility

is that the Sec24 mutants bind ER export competent cargo with a low affinity. Under conditions of non increased availability of ER export competent cargo (i.e. in conditions of non-overexpression of ERD2GFP), the Sec24 mutants are barely visible on ERES. However, under conditions of over-expression of cargo like ERD2GFP, a larger amount of mutated Sec24 and endogenous Sec24 are attracted onto ERES. Therefore, under these conditions Sec24 mutants become visible. A second hypothesis to explain this effect is that, in addition to the mutated residues, other residues involved in cargo signal motif binding were present. Under cargo over-expression conditions, the mutated Sec24 may be recruited through the other non-mutated residues. Finally, it is also possible that in conditions of increased availability of cargo that needs to be exported from the ER, a large number of SNAREs that facilitate ER export would accumulate at ERES. As a consequence, a larger number of Sec24 mutant proteins would be recruited to ERES in comparison to cells that do not overexpress ERD2GFP and would clearly accumulate at ERES in comparison to cells where the Sec24 mutants are expressed alone.

## 5. Conclusions

This work demonstrated that:

1. In plant cells Sec24 is distributed on the ERES. ERES and mobile Golgi are associated. This supports the mobile secretory unit model established by daSilva et al. (2004).
2. ERES integrity and ER export depend on the retrograde and anterograde pathways.
3. Sec24 is able to interact with the SNARE proteins Sed5 and Sec22 in plant cells. This may lead to cooperation among these proteins during the cargo selection process and ER export.
4. The Sec24 mutants, created on the basis of crystallographic evidence (Bi et al., 2002), have a lower ERES binding efficiency in comparison to wtSec24.

This work is innovative under several aspects. The research carried out for this work was based on the use of the COPII coat marker, Sec24. This marker, differently from the marker used in daSilva et al. (2004), a tobacco Sar1 isoform, is recruited visibly to ERES in absence of increased secretion of Golgi cargo. Therefore, Sec24 has allowed me to follow the dynamics of ERES in cells in conditions of non-induced and induced secretion. This work has also allowed me to support the mobile ERES model over the vacuum-cleaner model and the Stop-and-Go model. Moreover, my work is the first to report on the interaction of a COPII-coat component and SNARE in plant cells. Such an interaction could have been predicted on the basis of yeast literature. However, given the large differences in the

organization of the early secretory pathways of plant, mammals and yeast, it is important to test whether the COPII machinery has conserved features to operate at the Golgi/ER interface in these systems. Finally, to my knowledge, no studies have yet been published on the subcellular distribution of putative Sec24 mutants with reduced ability to bind SNAREs. Therefore my work could be used for future studies aimed at understanding how the Sec24/SNARE interaction takes place. In particular, whether the Sec24 mutants have a quantifiable decreased affinity for cargo or SNAREs has to be confirmed by further studies. In addition, it will be important to test the interaction between the Sec24 mutants and the different SNARE proteins involved in ER export as well as to identify other candidate sites in Sec24 responsible for cargo signal motif binding. This will aid our understanding of the control mediated by cargo and SNARE proteins on the assembly of COPII at ERES.

## 6. APPENDIX

Table A1 Plasmids, *A. tumefaciens* and *E. coli* strains, used in this work.

Plasmids	Resistance
pET 28b <sup>a</sup>	Kanamycin <sup>R</sup>
pGEX <sup>b</sup>	Ampicillin <sup>R</sup>
pVKH18EN6a <sup>c</sup>	Kanamycin <sup>R</sup> , Hygromycin <sup>R</sup>
pVKH18EN6b <sup>c</sup>	Kanamycin <sup>R</sup> , Hygromycin <sup>R</sup>
<i>Agrobacterium tumefaciens</i> strain	
GV3101 <sup>d</sup>	Gentamycin <sup>R</sup>
<i>Escherichia coli</i> strains	
MC1061 <sup>e</sup>	Streptomycin <sup>R</sup>
BL21 <sup>f</sup>	<i>E. coli</i> B F <sup>-</sup> dcm ompT hsdS(r <sub>B</sub> <sup>-</sup> m <sub>B</sub> <sup>-</sup> ) gal

(a) Novagen ([www.novagen.com](http://www.novagen.com)), (b) (Kaelin et al., 1992), (c) (Batoko et al., 2000), (d) Brandizzi lab's stock, (e) Invitrogen ([www.invitrogen.com](http://www.invitrogen.com)), (f) Stratagene ([www.stratagene.com](http://www.stratagene.com)).

Table A2 solutions. All the solutions were prepared as in (a) QIAGEN-QIAexpressionist; (b) Sambrook et al., 1989; (c) Thorpe and Kricka, 1986; (d) BD biosciences, glutathione resins user manual; (e) Lu and Hong, 2003.

<b>Solutions</b>	<b>Fomulations</b>
Sample buffer 5X <sup>a</sup>	0.225 M Tris-HCl, pH 6.8; 50 % glycerol; 5 % SDS; 0.05 % bromophenol blue; 0.25 M DTT
TFBI <sup>b</sup>	30 mM $KC_2H_3O_2$ , 100 mM RbCl, 10 mM $CaCl_2 \cdot 2H_2O$ , 50 mM $MnCl_2 \cdot 4H_2O$ , 15 % glycerol, pH 5.8 with 0.2 M $CH_3COOH$ .
TFBII <sup>b</sup>	10 mM MOPS, 10 mM RbCl, 75 mM $CaCl_2 \cdot 2H_2O$ , 15 % glycerol, pH 6.6 with 1M KOH.
50X TAE <sup>b</sup>	242 g/L Tris base, 57.1 mL/L glacial acetic acid, 37.2 $Na_2EDTA \cdot 2H_2O$
Loading buffer 10X <sup>b</sup>	35 % glycerol, 2.5 g/L Bromophenol blue in 10 X TAE



Coomassie brilliant blue staining solution <sup>b</sup>	0.1 % Coomassie brilliant blue R-250, 40 % ethanol, 10 % acetic acid.
Coomassie brilliant blue destaining solution <sup>b</sup>	40 % ethanol, 10 % acetic acid.
P1 <sup>a</sup>	1 mM EDTA, 50 mM TRIS, pH 8.0.
P2 <sup>a</sup>	0.2 N NaOH, 1 % SDS.
P3 <sup>a</sup>	11.5 % acetic acid, 3 M potassium acetate, pH 5.5.
5X SDS-PAGE running buffer <sup>b</sup>	30 g/L Tris base, 144 g/L glycine, 5 g/L SDS.
Blotting buffer <sup>b</sup>	3.03 g/L Tris base, 144 g/L glycine, 20 % v/v methanol.

<b>Solutions</b>	<b>Fomulations</b>
Ponceau S solution <sup>b</sup>	0.1 % w/v Ponceau S, 5 % v/v acetic acid
Blocking solution <sup>b</sup>	5 % (w/v) nonfat dry milk, 0.05 % tween 20, 0.02 % sodium azide in PBS.
Working solution <sup>b</sup>	1 % (w/v) nonfat dry milk, 0.05 % tween 20, 0.02 % sodium azide in PBS.
10X PBS <sup>b</sup>	87 g/L NaCl, 22.5 g/L Na <sub>2</sub> HPO <sub>4</sub> -2H <sub>2</sub> O, 2 g/L KH <sub>2</sub> PO <sub>4</sub> , pH 7.4.
ECL1 <sup>c</sup>	1 M Tris-HCl pH 8.5, 90 mM p-coumaric acid, 250 mM Luminol
ECL2 <sup>c</sup>	1 M Tris-HCl pH 8.5, 3 % H <sub>2</sub> O <sub>2</sub>
GST Extraction/lysis buffer (loading) <sup>d</sup>	140 mM NaCl; 10 mM Na <sub>2</sub> HPO <sub>4</sub> ; 1.8 mM KH <sub>2</sub> PO <sub>4</sub> (pH 7.5).
Elution buffer <sup>d</sup>	20 mM Glutathione in 50 mM Tris-HCl (pH 8.0).

NE buffer <sup>e</sup>	20 mM HEPES, pH 7.5, 100 mM NaCl, 10 mM EDTA, 5 mM MgCl <sub>2</sub>
NS buffer <sup>e</sup>	20 mM HEPES, pH 7.5, 100 mM NaCl, 5 mM MgCl <sub>2</sub>
Kanamycin	Stock solution in water 100 mg/mL, kept at -20°C.
Ampicillin	Stock solution in water 100 mg/mL, kept at -20°C.
Gentamycin	Stock solution in water 100 mg/mL, kept at -20°C.
IPTG	Stock solution in water 1 M, kept at -20°C.
IF	20 mM Na <sub>3</sub> (PO <sub>4</sub> ), 500 mM MES, 200 mM acetosyringone, 5 mg/mL glucose.

---

Table A3. Restriction endonucleases used in this work.

<b>Name</b>	<b>Supplier</b>	<b>addresses</b>
<i>Pfu</i>	Fermentas	<a href="http://www.fermentas.com">www.fermentas.com</a>
Ribonclease A	Fermentas	<a href="http://www.fermentas.com">www.fermentas.com</a>
T4 DNA ligase	Invitrogen	<a href="http://www.invitrogen.com">www.invitrogen.com</a>
<i>BamHI</i>	Fermentas	<a href="http://www.fermentas.com">www.fermentas.com</a>
<i>SacI</i>	Fermentas	<a href="http://www.fermentas.com">www.fermentas.com</a>

Table A4. Primers used in PCR reactions. All the primers were purchased from Invitrogen, desalted and at a 50 nmoles scale.

<b>Primer</b>	<b>Sequence</b>	<b>Restriction site</b>	<b>protein</b>
FB276	5'GGTGCTGGATCCATGGGTACGGAGAATCAGGGCTATCC	<i>Bam</i> HI	Sec24wt
FB278	3'GCGCCGGAGCTCGTTTTGTTGAACTTGGCGGTGAAG	<i>Sac</i> I	Sec24wt
LR6	5'CATAGCTCCAAGTGAAGCCATGGTTCGGCCTCCG		Sec24Y438A
LR7	3'CGGAGGCCGAACCATGGCTTCAGTTGGAGCTATG		Sec24Y438A
LR8	5'CTGCGTGGGAGGCGGCTATGCGAATAAGATGTG		Sec24V689A
LR9	3'CACATCTTATTCGCATAGCCGCCTCCCACGCAG		Sec24V689A
LR10	5'CCAAGTGGCTTTGGCATATACCGCCTCTTGTGG		Sec24L749A
LR11	3'CCACAAGAGGCGGTATATGCCAAAGCCACTTGG		Sec24L749A

(n.a.= non applicable because primers internal used for overlapping PCRs).

Table A5. Kits used in this work.

<b>Name</b>	<b>Supplier</b>	<b>addresses</b>
GFX PCR DNA and gel band purification	Amrsham Bioscences	<a href="http://www6.amershambiosciences.com">www6.amershambiosciences.com</a>
Glutathione S-transferase (GST)	BD biosciences	<a href="http://www.bdbiosciences.com">www.bdbiosciences.com</a>
Coomassie (Bradford) protein Assay Kit	Pierce	<a href="http://www.piercenet.com">www.piercenet.com</a>
Metal talon affinity resin	Qiagen	<a href="http://www.qiagen.com">www.qiagen.com</a>

Table A6. All the described media were prepared as in Sambrook et al. (1989).

<b>Medium</b>	<b>Formulation</b>
LB liquid	10 g/L bacto peptone-tryptone, 5 g/L yeast extract, 10g/l NaCl.
LB solid	10 g/L bacto peptone-tryptone, 5 g/L yeast extract, 10 g/L NaCl, 10 g/L agar.
YT	16 g/L bacto-tryptone, 10 g/L yeast extract, 5 g/L NaCl, pH 7.0.

Table A7 composition of PCR reactions

<b>Reagent</b>	<b>Quantity, for 200µl of reaction mixture</b>
Template DNA	1 µL
<i>Pfu</i> buffer (10x)+ MgSO <sub>4</sub> (25 mM)	20 µL
<i>Pfu</i> DNA Polymerase (Fermentas)	1 µL
Sense primer (50 pmol/µL)	0.6 µL
Antisense primer (50 pmol/µL)	0.6 µL
dNTP (100 mM)	4 µL
Sterile distilled H <sub>2</sub> O	172.8 µL

(Aliquoted in two tubes and overlaid with mineral oil).



Table A8. Solutions for preparing separating and stacking gels.

<b>Separating gel 10%</b>	<b>Final volume 10 mL</b>
dH <sub>2</sub> O	4.0 mL
30% acrylamide/bisacrylamide mix	3.3 mL
1.5M Tris (pH 8.8)	2.5 mL
10% SDS	0.1 mL
10% ammonium persulfate	0.1 mL
TEMED	0.004 mL

<b>Stacking gel 5%</b>	<b>Final volume 4 mL</b>
dH <sub>2</sub> O	2.7 mL
30% acrylamide/bisacrylamide mix	0.67 mL
1.5M Tris (pH 8.8)	0.5 mL
10% SDS	0.04 mL
10% ammonium persulfate	0.04 mL
TEMED	0.004 mL

## 7. REFERENCES

- Andreeva, A.V., Kutuzov, M.A., Evans, D.E., and Hawes, C.R.** (1998). Proteins involved in membrane transport between the ER and the Golgi apparatus: 21 putative plant homologues revealed by dbEST searching. *Cell Biol Int* **22**, 145-160.
- Andreeva, A.V., Zheng, H., Saint-Jore, C.M., Kutuzov, M.A., Evans, D.E., and Hawes, C.R.** (2000). Organization of transport from endoplasmic reticulum to Golgi in higher plants. *Biochem Soc Trans* **28**, 505-512.
- Antonny, B., and Schekman, R.** (2001). ER export: public transportation by the COPII coach. *Curr Opin Cell Biol* **13**, 438-443.
- Antonny, B., Madden, D., Hamamoto, S., Orci, L., and Schekman, R.** (2001). Dynamics of the COPII coat with GTP and stable analogues. *Nat Cell Biol* **3**, 531-537.
- Aridor, M., and Balch, W.E.** (2000). Kinase signaling initiates coat complex II (COPII) recruitment and export from the mammalian endoplasmic reticulum. *J Biol Chem* **275**, 35673-35676.
- Aridor, M., Bannykh, S.I., Rowe, T., and Balch, W.E.** (1995). Sequential coupling between COPII and COPI vesicle coats in endoplasmic reticulum to Golgi transport. *J Cell Biol* **131**, 875-893.
- Aridor, M., Bannykh, S.I., Rowe, T., and Balch, W.E.** (1999). Cargo can modulate COPII vesicle formation from the endoplasmic reticulum. *J Biol Chem* **274**, 4389-4399.
- Aridor, M., Weissman, J., Bannykh, S., Nuoffer, C., and Balch, W.E.** (1998). Cargo selection by the COPII budding machinery during export from the ER. *J Cell Biol* **141**, 61-70.
- Aridor, M., Fish, K.N., Bannykh, S., Weissman, J., Roberts, T.H., Lippincott-Schwartz, J., and Balch, W.E.** (2001). The Sar1 GTPase coordinates biosynthetic cargo selection with endoplasmic reticulum export site assembly. *J Cell Biol* **152**, 213-229.
- Barlowe, C.** (2002). COPII-dependent transport from the endoplasmic reticulum. *Curr Opin Cell Biol* **14**, 417-422.
- Barlowe, C.** (2003). Signals for COPII-dependent export from the ER: what's the ticket out? *Trends Cell Biol* **13**, 295-300.
- Barlowe, C., Orci, L., Yeung, T., Hosobuchi, M., Hamamoto, S., Salama, N., Rexach, M.F., Ravazzola, M., Amherdt, M., and Schekman, R.** (1994). COPII: a membrane coat formed by Sec proteins that drive vesicle budding from the endoplasmic reticulum. *Cell* **77**, 895-907.
- Batoko, H., Zheng, H.Q., Hawes, C., and Moore, I.** (2000). A rab1 GTPase is required for transport between the endoplasmic reticulum and golgi apparatus and for normal golgi movement in plants. *Plant Cell* **12**, 2201-2218.
- Bednarek, S.Y., Orci, L., and Schekman, R.** (1996). Traffic COPs and the formation of vesicle coats. *Trends Cell Biol* **6**, 468-473.

- Benghezal, M., Wasteneys, G.O., and Jones, D.A.** (2000). The C-terminal dilysine motif confers endoplasmic reticulum localization to type I membrane proteins in plants. *Plant Cell* **12**, 1179-1201.
- Bi, X., Corpina, R.A., and Goldberg, J.** (2002). Structure of the Sec23/24-Sar1 pre-budding complex of the COPII vesicle coat. *Nature* **419**, 271-277.
- Bigay, J., Gounon, P., Robineau, S., and Antonny, B.** (2003). Lipid packing sensed by ArfGAP1 couples COPI coat disassembly to membrane bilayer curvature. *Nature* **426**, 563-566.
- Boevink, P., Oparka, K., Santa Cruz, S., Martin, B., Betteridge, A., and Hawes, C.** (1998). Stacks on tracks: the plant Golgi apparatus traffics on an actin/ER network. *Plant J* **15**, 441-447.
- Bradford, M.M.** (1976). A rapid and sensitive method for the quantitation of microgram quantities of protein utilizing the principle of protein-dye binding. *Anal Biochem* **72**, 248-254.
- Brandizzi, F., Fricker, M., and Hawes, C.** (2002a). A greener world: the revolution in plant bioimaging. *Nat Rev Mol Cell Biol* **3**, 520-530.
- Brandizzi, F., Irons, S.L., Johansen, J., Kotzer, A., and Neumann, U.** (2004). GFP is the way to glow: bioimaging of the plant endomembrane system. *J Microsc* **214**, 138-158.
- Brandizzi, F., Frangne, N., Marc-Martin, S., Hawes, C., Neuhaus, J.M., and Paris, N.** (2002b). The destination for single-pass membrane proteins is influenced markedly by the length of the hydrophobic domain. *Plant Cell* **14**, 1077-1092.
- Chatre, L., Brandizzi, F., Hocquellet, A., Hawes, C., and Moreau, P.** (2005). Sec22 and Memb11 are v-SNAREs of the anterograde endoplasmic reticulum-Golgi pathway in tobacco leaf epidermal cells. *Plant Physiol* **139**, 1244-1254.
- Chen, D., Minger, S.L., Honer, W.G., and Whiteheart, S.W.** (1999). Organization of the secretory machinery in the rodent brain: distribution of the t-SNAREs, SNAP-25 and SNAP-23. *Brain Res* **831**, 11-24.
- Contreras, I., Ortiz-Zapater, E., Castilho, L.M., and Aniento, F.** (2000). Characterization of Cop I coat proteins in plant cells. *Biochem Biophys Res Commun* **273**, 176-182.
- Contreras, I., Yang, Y., Robinson, D.G., and Aniento, F.** (2004). Sorting signals in the cytosolic tail of plant p24 proteins involved in the interaction with the COPII coat. *Plant Cell Physiol* **45**, 1779-1786.
- Dascher, C., Ossig, R., Gallwitz, D., and Schmitt, H.D.** (1991). Identification and structure of four yeast genes (SLY) that are able to suppress the functional loss of YPT1, a member of the RAS superfamily. *Mol Cell Biol* **11**, 872-885.
- daSilva, L.L., Snapp, E.L., Denecke, J., Lippincott-Schwartz, J., Hawes, C., and Brandizzi, F.** (2004). Endoplasmic reticulum export sites and Golgi bodies behave as single mobile secretory units in plant cells. *Plant Cell* **16**, 1753-1771.
- Denecke, J., Botterman, J., and Deblaere, R.** (1990). Protein secretion in plant cells can occur via a default pathway. *Plant Cell* **2**, 51-59.

- Denzer, A.J., Nabholz, C.E., and Spiess, M.** (1995). Transmembrane orientation of signal-anchor proteins is affected by the folding state but not the size of the N-terminal domain. *Embo J* **14**, 6311-6317.
- Donaldson, J.G., Finazzi, D., and Klausner, R.D.** (1992a). Brefeldin A inhibits Golgi membrane-catalysed exchange of guanine nucleotide onto ARF protein. *Nature* **360**, 350-352.
- Donaldson, J.G., Kahn, R.A., Lippincott-Schwartz, J., and Klausner, R.D.** (1991). Binding of ARF and beta-COP to Golgi membranes: possible regulation by a trimeric G protein. *Science* **254**, 1197-1199.
- Donaldson, J.G., Cassel, D., Kahn, R.A., and Klausner, R.D.** (1992b). ADP-ribosylation factor, a small GTP-binding protein, is required for binding of the coatamer protein beta-COP to Golgi membranes. *Proc Natl Acad Sci U S A* **89**, 6408-6412.
- Duden, R., Hosobuchi, M., Hamamoto, S., Winey, M., Byers, B., and Schekman, R.** (1994). Yeast beta- and beta'-coat proteins (COP). Two coatamer subunits essential for endoplasmic reticulum-to-Golgi protein traffic. *J Biol Chem* **269**, 24486-24495.
- Ferro-Novick, S., and Jahn, R.** (1994). Vesicle fusion from yeast to man. *Nature* **370**, 191-193.
- Fitchette, A.C., Cabanes-Macheteau, M., Marvin, L., Martin, B., Satiat-Jeunemaitre, B., Gomord, V., Crooks, K., Lerouge, P., Faye, L., and Hawes, C.** (1999). Biosynthesis and immunolocalization of Lewis a-containing N-glycans in the plant cell. *Plant Physiol* **121**, 333-344.
- Gillingham, A.K., Pfeifer, A.C., and Munro, S.** (2002). CASP, the alternatively spliced product of the gene encoding the CCAAT-displacement protein transcription factor, is a Golgi membrane protein related to giantin. *Mol Biol Cell* **13**, 3761-3774.
- Giraud, C.G., and Maccioni, H.J.** (2003). Endoplasmic reticulum export of glycosyltransferases depends on interaction of a cytoplasmic dibasic motif with Sar1. *Mol Biol Cell* **14**, 3753-3766.
- Glick, B.S., and Malhotra, V.** (1998). The curious status of the Golgi apparatus. *Cell* **95**, 883-889.
- Gorelick, F.S., and Shugrue, C.** (2001). Exiting the endoplasmic reticulum. *Mol Cell Endocrinol* **177**, 13-18.
- Griffith, G.** (2000). Gut thoughts on the Golgi complex. *Traffic* **1**, 738-745.
- Hammond, A.T., and Glick, B.S.** (2000). Dynamics of transitional endoplasmic reticulum sites in vertebrate cells. *Mol Biol Cell* **11**, 3013-3030.
- Hampton, R.Y., Koning, A., Wright, R., and Rine, J.** (1996). In vivo examination of membrane protein localization and degradation with green fluorescent protein. *Proc Natl Acad Sci U S A* **93**, 828-833.
- Hanton, S.L., Matheson, L.A., and Brandizzi, F.** (2006). Seeking a way out: export of proteins from the plant endoplasmic reticulum. *Trends Plant Sci* **11**, 335-343.
- Hanton, S.L., Bortolotti, L.E., Renna, L., Stefano, G., and Brandizzi, F.** (2005a). Crossing the divide--transport between the endoplasmic reticulum and Golgi apparatus in plants. *Traffic* **6**, 267-277.

- Hanton, S.L., Chatre, L., Renna, L., Matheson, L.A., and Brandizzi, F.** (2007). De Novo Formation of Plant Endoplasmic Reticulum Export Sites Is Membrane Cargo-induced and Signal-mediated. *Plant Physiol.*
- Hanton, S.L., Renna, L., Bortolotti, L.E., Chatre, L., Stefano, G., and Brandizzi, F.** (2005b). Diacidic motifs influence the export of transmembrane proteins from the endoplasmic reticulum in plant cells. *Plant Cell* **17**, 3081-3093.
- Hardwick, K.G., and Pelham, H.R.** (1992). SED5 encodes a 39-kD integral membrane protein required for vesicular transport between the ER and the Golgi complex. *J Cell Biol* **119**, 513-521.
- Hawes, C., and Satiat-Jeunemaitre, B.** (2005). The plant Golgi apparatus--going with the flow. *Biochim Biophys Acta* **1744**, 93-107.
- Helms, J.B., and Rothman, J.E.** (1992). Inhibition by brefeldin A of a Golgi membrane enzyme that catalyses exchange of guanine nucleotide bound to ARF. *Nature* **360**, 352-354.
- Higuchi, R., Krummel, B., and Saiki, R.K.** (1988). A general method of in vitro preparation and specific mutagenesis of DNA fragments: study of protein and DNA interactions. *Nucleic Acids Res* **16**, 7351-7367.
- Hinners, I., Moschner, J., Nolte, N., and Hille-Rehfeld, A.** (1999). The orientation of membrane proteins determined in situ by immunofluorescence staining. *Anal Biochem* **276**, 1-7.
- Ho, S.N., Hunt, H.D., Horton, R.M., Pullen, J.K., and Pease, L.R.** (1989). Site-directed mutagenesis by overlap extension using the polymerase chain reaction. *Gene* **77**, 51-59.
- Hofte, H., and Chrispeels, M.J.** (1992). Protein sorting to the vacuolar membrane. *Plant Cell* **4**, 995-1004.
- Hong, W.** (2005). SNAREs and traffic. *Biochim Biophys Acta* **1744**, 120-144.
- Jackson, M.R., Nilsson, T., and Peterson, P.A.** (1993). Retrieval of transmembrane proteins to the endoplasmic reticulum. *J Cell Biol* **121**, 317-333.
- Jahn, R., Lang, T., and Sudhof, T.C.** (2003). Membrane fusion. *Cell* **112**, 519-533.
- Jurgens, G.** (2004). Membrane trafficking in plants. *Annu Rev Cell Dev Biol* **20**, 481-504.
- Kaelin, W.G., Jr., Krek, W., Sellers, W.R., DeCaprio, J.A., Ajchenbaum, F., Fuchs, C.S., Chittenden, T., Li, Y., Farnham, P.J., Blunar, M.A., and et al.** (1992). Expression cloning of a cDNA encoding a retinoblastoma-binding protein with E2F-like properties. *Cell* **70**, 351-364.
- Kapila, J., De Rycke, R., Van Montagu, M., Angenon, G., and** (1997). An Agrobacterium-mediated transient gene expression system for intact leaves. *Plant Sci* **122**, 101-108.
- Kappeler, F., Klopfenstein, D.R., Foguet, M., Paccaud, J.P., and Hauri, H.P.** (1997). The recycling of ERGIC-53 in the early secretory pathway. ERGIC-53 carries a cytosolic endoplasmic reticulum-exit determinant interacting with COPII. *J Biol Chem* **272**, 31801-31808.

- Klausner, R.D., Donaldson, J.G., and Lippincott-Schwartz, J.** (1992). Brefeldin A: insights into the control of membrane traffic and organelle structure. *J Cell Biol* **116**, 1071-1080.
- Kuehn, M.J., Herrmann, J.M., and Schekman, R.** (1998). COPII-cargo interactions direct protein sorting into ER-derived transport vesicles. *Nature* **391**, 187-190.
- Kuge, O., Dascher, C., Orci, L., Rowe, T., Amherdt, M., Plutner, H., Ravazzola, M., Tanigawa, G., Rothman, J.E., and Balch, W.E.** (1994). Sar1 promotes vesicle budding from the endoplasmic reticulum but not Golgi compartments. *J Cell Biol* **125**, 51-65.
- Laemmli, U.K.** (1970). Cleavage of structural proteins during the assembly of the head of bacteriophage T4. *Nature* **227**, 680-685.
- Latijhouwerrrs, M., Hawes, C., and Carvalho, C.** (2005). Holding it all together? Candidate proteins for the plant Golgi matrix. *Current opinion in Plant Biology* **8**, 1-8.
- Lee, M.C., Miller, E.A., Goldberg, J., Orci, L., and Schekman, R.** (2004). Bi-directional protein transport between the ER and Golgi. *Annu Rev Cell Dev Biol* **20**, 87-123.
- Lippincott-Schwartz, J., Roberts, T.H., and Hirschberg, K.** (2000). Secretory protein trafficking and organelle dynamics in living cells. *Annu Rev Cell Dev Biol* **16**, 557-589.
- Ma, D., Zerangue, N., Lin, Y.F., Collins, A., Yu, M., Jan, Y.N., and Jan, L.Y.** (2001). Role of ER export signals in controlling surface potassium channel numbers. *Science* **291**, 316-319.
- Mancias, J.D., and Goldberg, J.** (2005). Exiting the endoplasmic reticulum. *Traffic* **6**, 278-285.
- Matheson, L.A., Hanton, S.L., and Brandizzi, F.** (2006). Traffic between the plant endoplasmic reticulum and Golgi apparatus: to the Golgi and beyond. *Curr Opin Plant Biol* **9**, 601-609.
- Matsuoka, K., Schekman, R., Orci, L., and Heuser, J.E.** (2001). Surface structure of the COPII-coated vesicle. *Proc Natl Acad Sci U S A* **98**, 13705-13709.
- McMahon, H.T., and Mills, I.G.** (2004). COP and clathrin-coated vesicle budding: different pathways, common approaches. *Curr Opin Cell Biol* **16**, 379-391.
- Memon, A.R.** (2004). The role of ADP-ribosylation factor and SAR1 in vesicular trafficking in plants. *Biochim Biophys Acta* **1664**, 9-30.
- Miller, E., Antony, B., Hamamoto, S., and Schekman, R.** (2002). Cargo selection into COPII vesicles is driven by the Sec24p subunit. *Embo J* **21**, 6105-6113.
- Miller, E.A., Liu, Y., Barlowe, C., and Schekman, R.** (2005). ER-Golgi transport defects are associated with mutations in the Sed5p-binding domain of the COPII coat subunit, Sec24p. *Mol Biol Cell* **16**, 3719-3726.
- Miller, E.A., Beilharz, T.H., Malkus, P.N., Lee, M.C., Hamamoto, S., Orci, L., and Schekman, R.** (2003). Multiple cargo binding sites on the COPII subunit Sec24p ensure capture of diverse membrane proteins into transport vesicles. *Cell* **114**, 497-509.

- Miyawaki, A., Llopis, J., Heim, R., McCaffery, J.M., Adams, J.A., Ikura, M., and Tsien, R.Y.** (1997). Fluorescent indicators for Ca<sup>2+</sup> based on green fluorescent proteins and calmodulin. *Nature* **388**, 882-887.
- Mossessova, E., Bickford, L.C., and Goldberg, J.** (2003a). SNARE selectivity of the COPII coat. *Cell* **114**, 483-495.
- Mossessova, E., Corpina, R.A., and Goldberg, J.** (2003b). Crystal structure of ARF1\*Sec7 complexed with Brefeldin A and its implications for the guanine nucleotide exchange mechanism. *Mol Cell* **12**, 1403-1411.
- Nebenfür, A., Gallagher, L.A., Dunahay, T.G., Frohlick, J.A., Mazurkiewicz, A.M., Mechl, J.B., and Staehelin, L.A.** (1999). Stop-and-go movement of plant Golgi stacks are mediated by the actomyosin system. *Plant Physiology* **121**, 1127-1141.
- Neumann, U., Brandizzi, F., and Hawes, C.** (2003). Protein transport in plant cells: in and out of the Golgi. *Ann Bot (Lond)* **92**, 167-180.
- Newman, A.P., Shim, J., and Ferro-Novick, S.** (1990). BET1, BOS1, and SEC22 are members of a group of interacting yeast genes required for transport from the endoplasmic reticulum to the Golgi complex. *Mol Cell Biol* **10**, 3405-3414.
- Nie, Z., Hirsch, D.S., and Randazzo, P.A.** (2003). Arf and its many interactors. *Curr Opin Cell Biol* **15**, 396-404.
- Nishimura, N., and Balch, W.E.** (1997). A di-acidic signal required for selective export from the endoplasmic reticulum. *Science* **277**, 556-558.
- Nishimura, N., Bannykh, S., Slabough, S., Matteson, J., Altschuler, Y., Hahn, K., and Balch, W.E.** (1999). A di-acidic (DXE) code directs concentration of cargo during export from the endoplasmic reticulum. *J Biol Chem* **274**, 15937-15946.
- Ojakian, G.K., Nelson, W.J., and Beck, K.A.** (1997). Mechanisms for de novo biogenesis of an apical membrane compartment in groups of simple epithelial cells surrounded by extracellular matrix. *J Cell Sci* **110 ( Pt 22)**, 2781-2794.
- Orci, L., Ravazzola, M., Meda, P., Holcomb, C., Moore, H.P., Hicke, L., and Schekman, R.** (1991). Mammalian Sec23p homologue is restricted to the endoplasmic reticulum transitional cytoplasm. *Proc Natl Acad Sci U S A* **88**, 8611-8615.
- Palade, G.** (1975). Intracellular aspects of the process of protein synthesis. *Science* **189**, 347-358.
- Palmer, D.J., Helms, J.B., Beckers, C.J., Orci, L., and Rothman, J.E.** (1993). Binding of coatomer to Golgi membranes requires ADP-ribosylation factor. *J Biol Chem* **268**, 12083-12089.
- Parlati, F., McNew, J.A., Fukuda, R., Miller, R., Sollner, T.H., and Rothman, J.E.** (2000). Topological restriction of SNARE-dependent membrane fusion. *Nature* **407**, 194-198.
- Parlati, F., Varlamov, O., Paz, K., McNew, J.A., Hurtado, D., Sollner, T.H., and Rothman, J.E.** (2002). Distinct SNARE complexes mediating membrane fusion in Golgi transport based on combinatorial specificity. *Proc Natl Acad Sci U S A* **99**, 5424-5429.

- Peng, R., Grabowski, R., De Antoni, A., and Gallwitz, D.** (1999). Specific interaction of the yeast cis-Golgi syntaxin Sed5p and the coat protein complex II component Sec24p of endoplasmic reticulum-derived transport vesicles. *Proc Natl Acad Sci U S A* **96**, 3751-3756.
- Phillipson, B.A., Pimpl, P., daSilva, L.L., Crofts, A.J., Taylor, J.P., Movafeghi, A., Robinson, D.G., and Denecke, J.** (2001). Secretory bulk flow of soluble proteins is efficient and COPII dependent. *Plant Cell* **13**, 2005-2020.
- Pimpl, P., Movafeghi, A., Coughlan, S., Denecke, J., Hillmer, S., and Robinson, D.G.** (2000). In situ localization and in vitro induction of plant COPI-coated vesicles. *Plant Cell* **12**, 2219-2236.
- Pratelli, R., Sutter, J.U., and Blatt, M.R.** (2004). A new catch in the SNARE. *Trends Plant Sci* **9**, 187-195.
- Presley, J.F., Cole, N.B., Schroer, T.A., Hirschberg, K., Zaal, K.J., and Lippincott-Schwartz, J.** (1997). ER-to-Golgi transport visualized in living cells. *Nature* **389**, 81-85.
- Preuss, D., Mulholland, J., Franzusoff, A., Segev, N., and Botstein, D.** (1992). Characterization of the *Saccharomyces* Golgi complex through the cell cycle by immunoelectron microscopy. *Mol Biol Cell* **3**, 789-803.
- Puertollano, R., Randazzo, P.A., Presley, J.F., Hartnell, L.M., and Bonifacino, J.S.** (2001). The GGAs promote ARF-dependent recruitment of clathrin to the TGN. *Cell* **105**, 93-102.
- Rambourg, A., and Clermont, Y.** (1990). Three-dimensional electron microscopy: structure of the Golgi apparatus. *Eur J Cell Biol* **51**, 189-200.
- Renna, L., Hanton, S.L., Stefano, G., Bortolotti, L., Misra, V., and Brandizzi, F.** (2005). Identification and characterization of AtCASP, a plant transmembrane Golgi matrix protein. *Plant Mol Biol* **58**, 109-122.
- Roberg, K.J., Crotwell, M., Espenshade, P., Gimeno, R., and Kaiser, C.A.** (1999). LST1 is a SEC24 homologue used for selective export of the plasma membrane ATPase from the endoplasmic reticulum. *J Cell Biol* **145**, 659-672.
- Rose, J.K., and Doms, R.W.** (1988). Regulation of protein export from the endoplasmic reticulum. *Annu Rev Cell Biol* **4**, 257-288.
- Rossanese, O.W., Soderholm, J., Bevis, B.J., Sears, I.B., O'Connor, J., Williamson, E.K., and Glick, B.S.** (1999). Golgi structure correlates with transitional endoplasmic reticulum organization in *Pichia pastoris* and *Saccharomyces cerevisiae*. *J Cell Biol* **145**, 69-81.
- Rothman, J.E.** (1994). Mechanisms of intracellular protein transport. *Nature* **372**, 55-63.
- Saint-Jore, C.M., Evins, J., Batoko, H., Brandizzi, F., Moore, I., and Hawes, C.** (2002). Redistribution of membrane proteins between the Golgi apparatus and endoplasmic reticulum in plants is reversible and not dependent on cytoskeletal networks. *Plant J* **29**, 661-678.
- Sanderfoot, A.A., Assaad, F.F., and Raikhel, N.V.** (2000). The Arabidopsis genome. An abundance of soluble N-ethylmaleimide-sensitive factor adaptor protein receptors. *Plant Physiol* **124**, 1558-1569.



- Satiat-Jeunemaitre, B., and Hawes, C.** (1992). Redistribution of a Golgi glycoprotein in plant cells treated with Brefeldin A. *Journal of Cell Science* **103**, 1153-1166.
- Sato, K., and Nakano, A.** (2005). Reconstitution of cargo-dependent COPII coat assembly on proteoliposomes. *Methods Enzymol* **404**, 83-94.
- Schekman, R., and Orci, L.** (1996). Coat proteins and vesicle budding. *Science* **271**, 1526-1533.
- Seemann, J., Jokitalo, E., Pypaert, M., and Warren, G.** (2000). Matrix proteins can generate the higher order architecture of the Golgi apparatus. *Nature* **407**, 1022-1026.
- Sevier, C.S., Weisz, O.A., Davis, M., and Machamer, C.E.** (2000). Efficient export of the vesicular stomatitis virus G protein from the endoplasmic reticulum requires a signal in the cytoplasmic tail that includes both tyrosine-based and di-acidic motifs. *Mol Biol Cell* **11**, 13-22.
- Shima, D.T., Cabrera-Poch, N., Pepperkok, R., and Warren, G.** (1998). An ordered inheritance strategy for the Golgi apparatus: visualization of mitotic disassembly reveals a role for the mitotic spindle. *J Cell Biol* **141**, 955-966.
- Shimoni, Y., Kurihara, T., Ravazzola, M., Amherdt, M., Orci, L., and Schekman, R.** (2000). Lst1p and Sec24p cooperate in sorting of the plasma membrane ATPase into COPII vesicles in *Saccharomyces cerevisiae*. *J Cell Biol* **151**, 973-984.
- Shorter, J., and Warren, G.** (2002). Golgi architecture and inheritance. *Annu Rev Cell Dev Biol* **18**, 379-420.
- Slusarewicz, P., Nilsson, T., Hui, N., Watson, R., and Warren, G.** (1994). Isolation of a matrix that binds medial Golgi enzymes. *J Cell Biol* **124**, 405-413.
- Sollner, T., Bennett, M.K., Whiteheart, S.W., Scheller, R.H., and Rothman, J.E.** (1993). A protein assembly-disassembly pathway in vitro that may correspond to sequential steps of synaptic vesicle docking, activation, and fusion. *Cell* **75**, 409-418.
- Springer, S., and Schekman, R.** (1998). Nucleation of COPII vesicular coat complex by endoplasmic reticulum to Golgi vesicle SNAREs. *Science* **281**, 698-700.
- Springer, S., Spang, A., and Schekman, R.** (1999). A primer on vesicle budding. *Cell* **97**, 145-148.
- Staelin, L.A.** (1997). The plant ER: a dynamic organelle composed of a large number of discrete functional domains. *Plant J* **11**, 1151-1165.
- Stefano, G., Renna, L., Chatre, L., Hanton, S.L., Moreau, P., Hawes, C., and Brandizzi, F.** (2006). In tobacco leaf epidermal cells, the integrity of protein export from the endoplasmic reticulum and of ER export sites depends on active COPI machinery. *Plant J* **46**, 95-110.
- Stephens, D.J., and Pepperkok, R.** (2004). Differential effects of a GTP-restricted mutant of Sar1p on segregation of cargo during export from the endoplasmic reticulum. *J Cell Sci* **117**, 3635-3644.
- Stephens, D.J., Lin-Marq, N., Pagano, A., Pepperkok, R., and Paccaud, J.P.** (2000). COPI-coated ER-to-Golgi transport complexes segregate from

- COPII in close proximity to ER exit sites. *J Cell Sci* **113** ( Pt 12), 2177-2185.
- Storrie, B., White, J., Rottger, S., Stelzer, E.H., Suganuma, T., and Nilsson, T.** (1998). Recycling of golgi-resident glycosyltransferases through the ER reveals a novel pathway and provides an explanation for nocodazole-induced Golgi scattering. *J Cell Biol* **143**, 1505-1521.
- Subramanian, K., and Meyer, T.** (1997). Calcium-induced restructuring of nuclear envelope and endoplasmic reticulum calcium stores. *Cell* **89**, 963-971.
- Takeuchi, M., Ueda, T., Yahara, N., and Nakano, A.** (2002). Arf1 GTPase plays roles in the protein traffic between the endoplasmic reticulum and the Golgi apparatus in tobacco and Arabidopsis cultured cells. *Plant J* **31**, 499-515.
- Takeuchi, M., Ueda, T., Sato, K., Abe, H., Nagata, T., and Nakano, A.** (2000). A dominant negative mutant of sar1 GTPase inhibits protein transport from the endoplasmic reticulum to the Golgi apparatus in tobacco and Arabidopsis cultured cells. *Plant J* **23**, 517-525.
- Teal, S.B., Hsu, V.W., Peters, P.J., Klausner, R.D., and Donaldson, J.G.** (1994). An activating mutation in ARF1 stabilizes coatamer binding to Golgi membranes. *J Biol Chem* **269**, 3135-3138.
- Thyberg, J., and Moskalewski, S.** (1985). Microtubules and the organization of the Golgi complex. *Exp Cell Res* **159**, 1-16.
- Tsien, R.Y.** (1998). The green fluorescent protein. *Annu Rev Biochem* **67**, 509-544.
- Uemura, T., Ueda, T., Ohniwa, R.L., Nakano, A., Takeyasu, K., and Sato, M.H.** (2004). Systematic analysis of SNARE molecules in Arabidopsis: dissection of the post-Golgi network in plant cells. *Cell Struct Funct* **29**, 49-65.
- Ungar, D., and Hughson, F.M.** (2003). SNARE protein structure and function. *Annu Rev Cell Dev Biol* **19**, 493-517.
- Vasudevan, C., Han, W., Tan, Y., Nie, Y., Li, D., Shome, K., Watkins, S.C., Levitan, E.S., and Romero, G.** (1998). The distribution and translocation of the G protein ADP-ribosylation factor 1 in live cells is determined by its GTPase activity. *J Cell Sci* **111** ( Pt 9), 1277-1285.
- Vitale, A., and Denecke, J.** (1999). The endoplasmic reticulum-gateway of the secretory pathway. *Plant Cell* **11**, 615-628.
- Votsmeier, C., and Gallwitz, D.** (2001). An acidic sequence of a putative yeast Golgi membrane protein binds COPII and facilitates ER export. *Embo J* **20**, 6742-6750.
- Ward, T.H., Polishchuk, R.S., Caplan, S., Hirschberg, K., and Lippincott-Schwartz, J.** (2001). Maintenance of Golgi structure and function depends on the integrity of ER export. *J Cell Biol* **155**, 557-570.
- Waters, M.G., Serafini, T., and Rothman, J.E.** (1991). 'Coatamer': a cytosolic protein complex containing subunits of non-clathrin-coated Golgi transport vesicles. *Nature* **349**, 248-251.
- Watson, P., Townley, A.K., Koka, P., Palmer, K.J., and Stephens, D.J.** (2006). Sec16 Defines Endoplasmic Reticulum Exit Sites and is Required for Secretory Cargo Export in Mammalian Cells. *Traffic*.

- Weber, T., Zemelman, B.V., McNew, J.A., Westermann, B., Gmachl, M., Parlati, F., Sollner, T.H., and Rothman, J.E.** (1998). SNAREpins: minimal machinery for membrane fusion. *Cell* **92**, 759-772.
- Wennerberg, K., Rossman, K.L., and Der, C.J.** (2005). The Ras superfamily at a glance. *J Cell Sci* **118**, 843-846.
- Wessels, H.P., and Spiess, M.** (1988). Insertion of a multispanning membrane protein occurs sequentially and requires only one signal sequence. *Cell* **55**, 61-70.
- Wooding, S., and Pelham, H.R.** (1998). The dynamics of golgi protein traffic visualized in living yeast cells. *Mol Biol Cell* **9**, 2667-2680.
- Xu, J., and Scheres, B.** (2005). Dissection of Arabidopsis ADP-RIBOSYLATION FACTOR 1 function in epidermal cell polarity. *Plant Cell* **17**, 525-536.
- Yang, Y.D., Elamawi, R., Bubeck, J., Pepperkok, R., Ritzenthaler, C., and Robinson, D.G.** (2005). Dynamics of COPII vesicles and the Golgi apparatus in cultured *Nicotiana tabacum* BY-2 cells provides evidence for transient association of Golgi stacks with endoplasmic reticulum exit sites. *Plant Cell* **17**, 1513-1531.
- Yoshihisa, T., Barlowe, C., and Schekman, R.** (1993). Requirement for a GTPase-activating protein in vesicle budding from the endoplasmic reticulum. *Science* **259**, 1466-1468.
- Zaal, K.J., Smith, C.L., Polishchuk, R.S., Altan, N., Cole, N.B., Ellenberg, J., Hirschberg, K., Presley, J.F., Roberts, T.H., Siggia, E., Phair, R.D., and Lippincott-Schwartz, J.** (1999). Golgi membranes are absorbed into and reemerge from the ER during mitosis. *Cell* **99**, 589-601.
- Zeeh, J.C., Zeghouf, M., Grauffel, C., Guibert, B., Martin, E., Dejaegere, A., and Cherfils, J.** (2006). Dual specificity of the interfacial inhibitor brefeldin A for arf proteins and sec7 domains. *J Biol Chem* **281**, 11805-11814.
- Zhu, Y., Traub, L.M., and Kornfeld, S.** (1998). ADP-ribosylation factor 1 transiently activates high-affinity adaptor protein complex AP-1 binding sites on Golgi membranes. *Mol Biol Cell* **9**, 1323-1337.